| REPORT DOCUMENTATION PAGE | | READ INSTRUCTIONS BEFORE COMPLETING FORM |
|---|---|---|
| 1. REPORT NUMBER<br>DTNSRDC-81/018 | 2. GOVT ACCESSION NO.<br>AD-A107 081 | 3. RECIPIENT'S CATALOG NUMBER |
| 4. TITLE (and Subtitle)<br>STRUCTURAL ANALYSIS METHODS AND ELASTIC PROPERTY DETERMINATION FOR LAMINATED COMPOSITES. | | 5. TYPE OF REPORT & PERIOD COVERED<br>Research and Development/ Final Report. |
| | | 6. PERFORMING ORG. REPORT NUMBER |
| 7. AUTHOR(s)<br>Milton O. Critchfield | | 8. CONTRACT OR GRANT NUMBER(s) |
| 9. PERFORMING ORGANIZATION NAME AND ADDRESS<br>David W. Taylor Naval Ship Research and Development Center<br>Bethesda, Maryland 20084 | | 10. PROGRAM ELEMENT, PROJECT, TASK AREA & WORK UNIT NUMBERS<br>(See reverse side) |
| 11. CONTROLLING OFFICE NAME AND ADDRESS<br>Naval Sea Systems Command<br>Washington, D.C. 20362 | | 12. REPORT DATE<br>August 1981 |
| | | 13. NUMBER OF PAGES<br>90 |
| 14. MONITORING AGENCY NAME & ADDRESS(if different from Controlling Office) | | 15. SECURITY CLASS. (of this report)<br>UNCLASSIFIED |
| | | 15a. DECLASSIFICATION/DOWNGRADING SCHEDULE |

16. DISTRIBUTION STATEMENT (of this Report)

APPROVED FOR PUBLIC RELEASE: DISTRIBUTION UNLIMITED

17. DISTRIBUTION STATEMENT (of the abstract entered in Block 20, if different from Report)

18. SUPPLEMENTARY NOTES

19. KEY WORDS (Continue on reverse side if necessary and identify by block number)

Structural analysis, laminated composites, laminated beams, columns, ship structures, marine application, laminated plates, elastic properties, stiffness properties, elastic constants, hybrid structures, stress, deflection, bending, buckling, vibration, finite-element method, computer programs,
(Continued on reverse side)

20. ABSTRACT (Continue on reverse side if necessary and identify by block number)

Recent applications of laminated composites to ship structural components have highlighted both the analytical complexities involved and the need for providing the structural designer and analyst with appropriate laminate analysis methods. To this end, three types of analytical methods, traditionally applied to metallic ship structural components, have been extended to the analysis of laminated composites; procedures for their implementation are

(Continued on reverse side)

DD FORM 1473 EDITION OF 1 NOV 65 IS OBSOLETE
1 JAN 73
S/N 0102-LF-014-6601

(Block 10)

Program Element 62543N
Project 23556
Task Area SF-434-003-91
Work Unit 1730-610

(Block 19 continued)

classical analysis, test results, strength of materials, NASTRAN, experimental methods, anisotropic materials, orthotropic materials

(Block 20 continued)

discussed. These methods include (a) strength-of-materials techniques for laminated beam and column members, (b) classical analysis methods for the bending, buckling, and vibration of laminated plating, and (c) finite-element techniques for either individual laminated components or more complex hybrid structures. Finite-element approaches are discussed for investigating both the in-plane stresses in the individual layers of a laminate and the interlaminar shear and normal stresses which frequently govern near discontinuities in laminate cross sections. The use of these three analysis techniques necessitates that laminated composite components be analyzed as nonlaminated components having equivalent stiffness during in-plane axial and shear and out-of-plane bending responses. Three kinds of equivalent elastic properties for laminates are defined, and methods are presented for calculating each of them. Since these computational procedures may be quite lengthy for laminates with more than a few layers, a computer program is referenced which automates the procedures. Lastly, the effectiveness of different methods for laminate stiffness and stress analysis was investigated by comparing analytical and test results for a composite box beam having graphite epoxy flanges. Good agreement between analytical and test results provides encouragement for the further application of these methods.

| Accession For | |
|---|---|
| NTIS GRA&I | X |
| DTIC TAB | ☐ |
| Unannounced | ☐ |
| Justification | |

By
Distribution/
Availability Codes

| Dist | Avail and/or Special |
|---|---|
| A | |

DTIC
S ELECTE D
SEP 1 1 1981
D

## TABLE OF CONTENTS

## LIST OF FIGURES

LIST OF TABLES

## NOTATION

| | |
|---|---|
| A,B,D | Extensional, coupling, and bending stiffness matrices, respectively, for laminated plates |
| A*,B*,D* | Extensional, coupling, and bending stiffness matrices, respectively, for equivalent nonlaminated plates |
| $A_{ij}, B_{ij}, D_{ij}$ | Elements of matrices A, B, and D defined above (i and j take on integer values of 1, 2, and 6) |
| $\overline{A}_{ij}, \overline{D}_{ij}$ | Elements of inverted A and D matrices, respectively |
| a | Long side dimension of laminated plate |
| b | Short side dimension of laminated plate (also the width of laminated beam or column of rectangular cross section) |
| $b_1$ | Width of laminated flange element of hybrid beam ($b_1$ is also used for the width of an equivalent nonlaminated flange having an equivalent Young's modulus $E_f$) |
| $b_2$ | Width of a nonlaminated flange having an equivalent Young's modulus identical to the web modulus $E_w$ of the hybrid beam |
| $E_1, E_2$ | Young's moduli of individual lamina or layer in the "1" and "2" directions (along and normal to fibers, respectively) |
| $E_x, E_y$ | Young's moduli of laminate in x and y directions, respectively |
| $E_b$ | Effective Young's modulus of laminate under bending, or linearly varying strain, condition |
| $E_f$ | Equivalent Young's modulus for laminated flange element of hybrid beam |
| $E_w$ | Young's modulus for isotropic and homogeneous web element of hybrid beam |
| $G_{12}$ | Shear modulus of lamina with respect to the "1" and "2" directions |
| $G_{ij}$ | NASTRAN notation for the reduced stiffnesses $Q_{ij}$ (defined below-- not to be confused with the shear moduli, such as $G_{12}$ above, as explained in the report) |
| $G_{xy}$ | Shear modulus of laminate with respect to xy plane (the plane of the laminate) |
| h | Depth of laminated and equivalent nonlaminated beam or plate |

| | |
|---|---|
| $k_x, k_y, k_{xy}$ | Out-of-plane curvatures of the middle surface of the laminate |
| $M_x, M_y$ | Laminate moments, per unit width, associated with bending in the x and y directions, respectively |
| $M_{xy}$ | Laminate twisting moment per unit width |
| m,n | Integers, as defined in the report |
| $N_x, N_y$ | Laminate in-plane axial or normal forces, per unit width, in the x and y directions, respectively |
| $N_{xy}$ | Laminate in-plane shear force per unit width in xy plane |
| $P_0$ | Lateral pressure loading (force per unit area) on laminated plate |
| $Q_{ij}$ | Reduced stiffness for individual lamina with respect to material directions (parallel and normal to fibers) |
| $\overline{Q}_{ij}$ | Reduced stiffness $Q_{ij}$ for lamina after transformation to overall laminate x, y directions |
| $Q^*_{ij}$ | Overall laminate reduced stiffness |
| $Q^*_{ij(m)}, Q^*_{ij(b)}$ | Laminate reduced stiffnesses associated with membrane and bending behavior, respectively |
| w | Deflection of laminated plate |
| x,y,z | Right-handed laminate coordinate axes where x and y lie in the plane of the laminate and the z axis is normal to the plane |
| $\gamma_{xy}, \gamma_{zx}, \gamma_{zy}$ | Shearing strains in xy, zx, and zy planes, respectively |
| $\epsilon_x, \epsilon_y, \epsilon_z$ | Normal strains in x, y, and z directions, respectively, of laminate |
| $\eta_{x,xy}, \eta_{y,xy}$ | Coefficients of mutual influence of the first kind |
| $\eta_{xy,x}, \eta_{xy,y}$ | Coefficients of mutual influence of the second kind |
| $\theta$ | Angle of transformation between "1" axis (along the fibers) for individual lamina and the laminate x axis) |

| | |
|---|---|
| $\lambda$ | Half wavelength of laminate buckle |
| $\nu_{xy}, \nu_{yx}$ | Poisson's ratios |
| $\rho$ | Mass density of laminate |
| $\sigma_{cr}$ | Buckling stress for laminated plate (specially orthotropic or cross-ply type) |
| $\sigma_x, \sigma_y, \sigma_z$ | Normal stresses in x, y, and z directions, respectively, of laminate |
| $\tau_{xy}, \tau_{zx}, \tau_{zy}$ | Shear stresses in xy, zx, and zy planes of laminate |
| $\omega$ | Natural frequency of vibration of laminated plate |

## ABBREVIATIONS AND DEFINITIONS

| | |
|---|---|
| CQDMEM | Quadrilateral membrane element in NASTRAN |
| CQUAD1 | Quadrilateral membrane and bending element in NASTRAN |
| G/E (or GR/EP) | Graphite/Epoxy |
| kip | Thousands of |
| MAT2 | NASTRAN material property card |
| NASTRAN | A computer program used to perform finite-element analysis |
| PQUAD1 | NASTRAN property card |
| VPI | Virginia Polytechnic Institute |
| 2D | Two dimensional |
| 3D | Three dimensional |

## ABSTRACT

Recent applications of laminated composites to ship structural components have highlighted both the analytical complexities involved and the need for providing the structural designer and analyst with appropriate laminate analysis methods. To this end, three types of analytical methods, traditionally applied to metallic ship structural components, have been extended to the analysis of laminated composites; procedures for their implementation are discussed. These methods include (a) strength-of-materials techniques for laminated beam and column members, (b) classical analysis methods for the bending, buckling, and vibration of laminated plating, and (c) finite-element techniques for either individual laminated components or more complex hybrid structures. Finite-element approaches are discussed for investigating both the in-plane stresses in the individual layers of a laminate and the interlaminar shear and normal stresses which frequently govern near discontinuities in laminate cross sections. The use of these three analysis techniques necessitates that laminated composite components be analyzed as nonlaminated components having equivalent stiffness during in-plane axial and shear and out-of-plane bending responses. Three kinds of equivalent elastic properties for laminates are defined, and methods are presented for calculating each of them. Since these computational procedures may be quite lengthy for laminates with more than a few layers, a computer program is referenced which automates the procedures. Lastly, the effectiveness of different methods for laminate stiffness and stress analysis was investigated by comparing analytical and test results for a composite box beam having graphite epoxy flanges. Good agreement between analytical and test results provides encouragement for the further application of these methods.

## ADMINISTRATIVE INFORMATION

## INTRODUCTION

Composite materials have been employed in aerospace structures for many years and are now receiving increased consideration for application to ship structural

components. Two recent experimental applications include (a) a box beam simulation of the forward foil and (b) aft foil flap component (Figures 1 and 2) of the PCH-1 hydrofoil.[1]*,[2],**
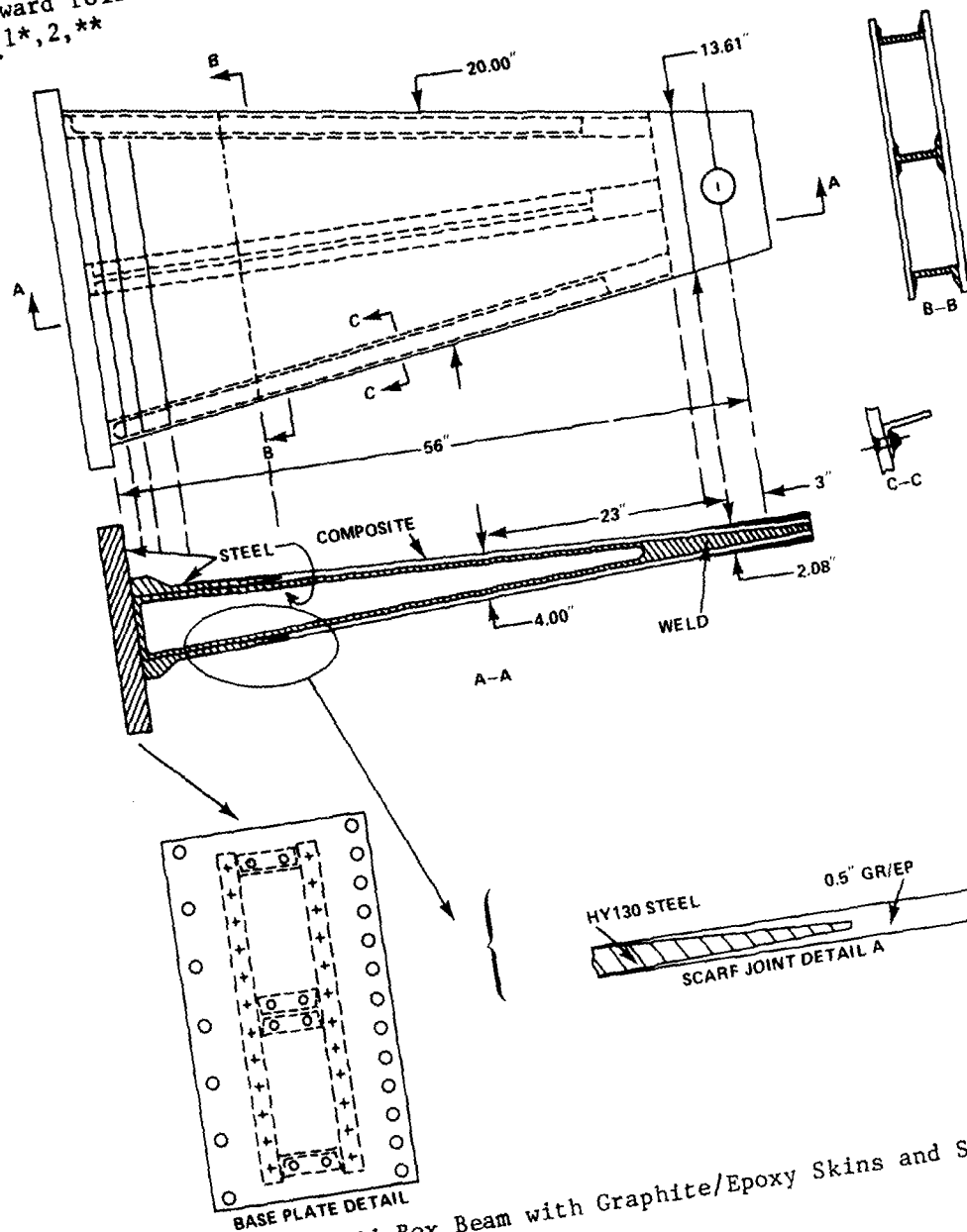


Figure 1 – Hybrid Box Beam with Graphite/Epoxy Skins and Steel Skeleton

_____

*A complete listing of references is given on page 79.

**W.P. Couch, "Advanced Composite Box Beam: Laboratory Evaluation and Technology Assessment Plan," reported informally as enclosure (1) to DTNSRDC ltr 77-173-191, 30 Sep 1977.

2
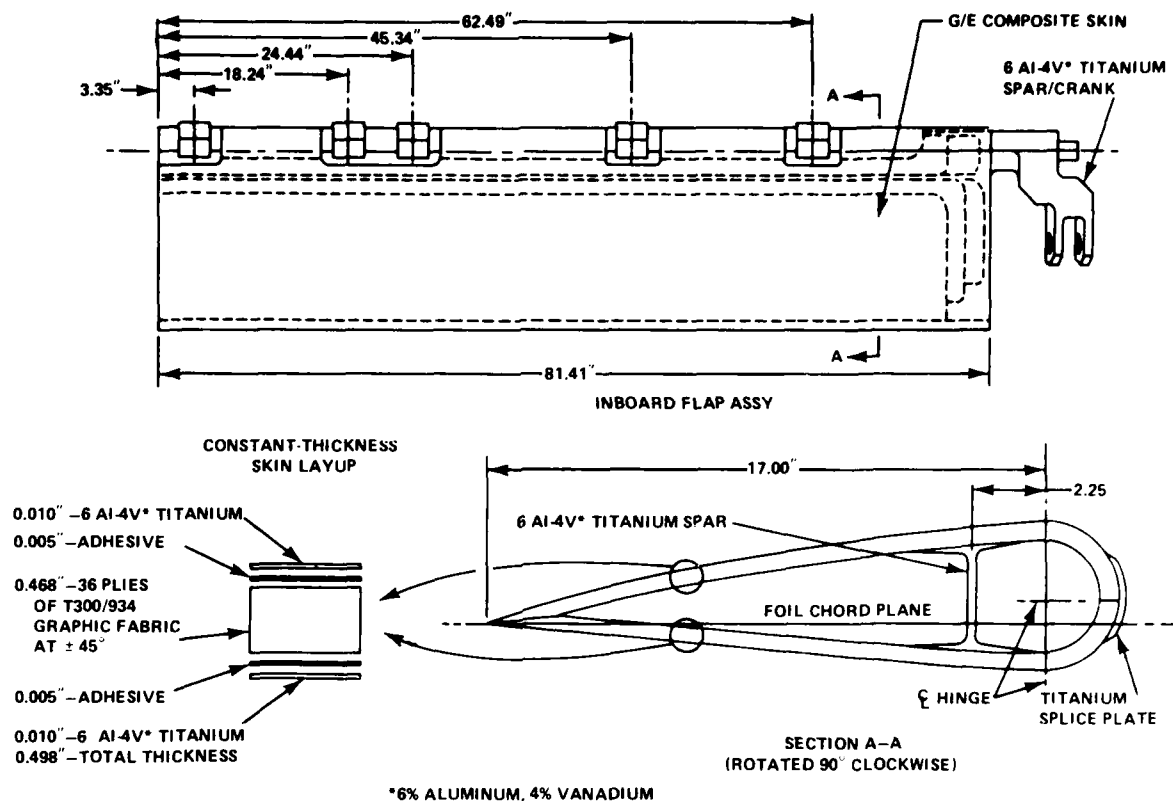
Figure 2 – Composite Foil Flap Component

In classifying composite materials, three commonly accepted types are recognized: laminated composites, fibrous composites, and particulate composites. This report is concerned with the first type, the laminated composites, which are normally fabricated by stacking and orienting layers of fiber-imbedded cloth or tape in preferred directions to achieve desired strength and stiffness properties. An example of a four-layer laminate is shown in Figure 3.

As illustrated in Figure 4, existing and potential applications of laminated composites in ship structural components include: (a) laminated beams and columns, (b) laminated plating used as the flanges of beams or columns, (c) laminated plates, and laminated plating for (d) panels and grillages, and (e) the skins of box-type structures.

IMBEDDED FIBERS

MATRIX MATERIAL
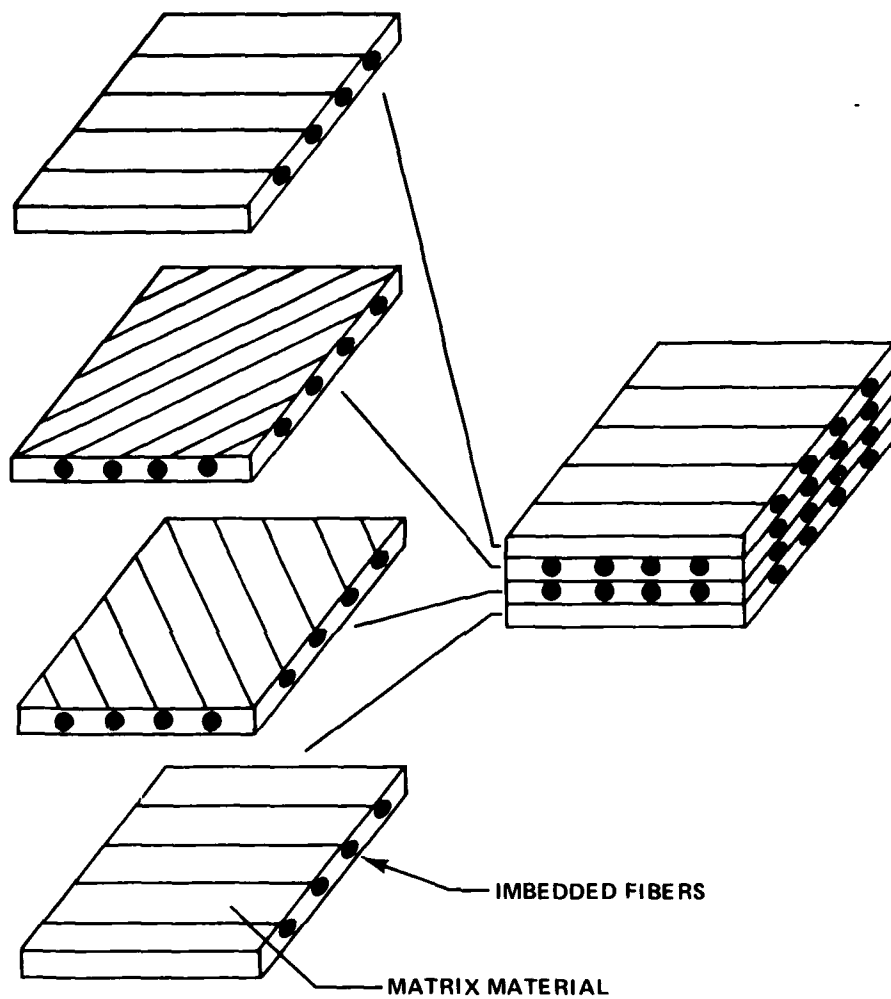
Figure 3 - Arrangement of Typical Four-Layer Laminate Composite

(A)                                **LAMINATED BEAM/COLUMN**

(B)                                **LAMINATED PLATE AS FLANGE OF BEAM AND/OR COLUMN**

(C)                                **LAMINATED PLATES**

(D)                                **HYBRID 2D PANELS AND GRILLAGES**

(E)                                **HYBRID 3D STRUCTURES**
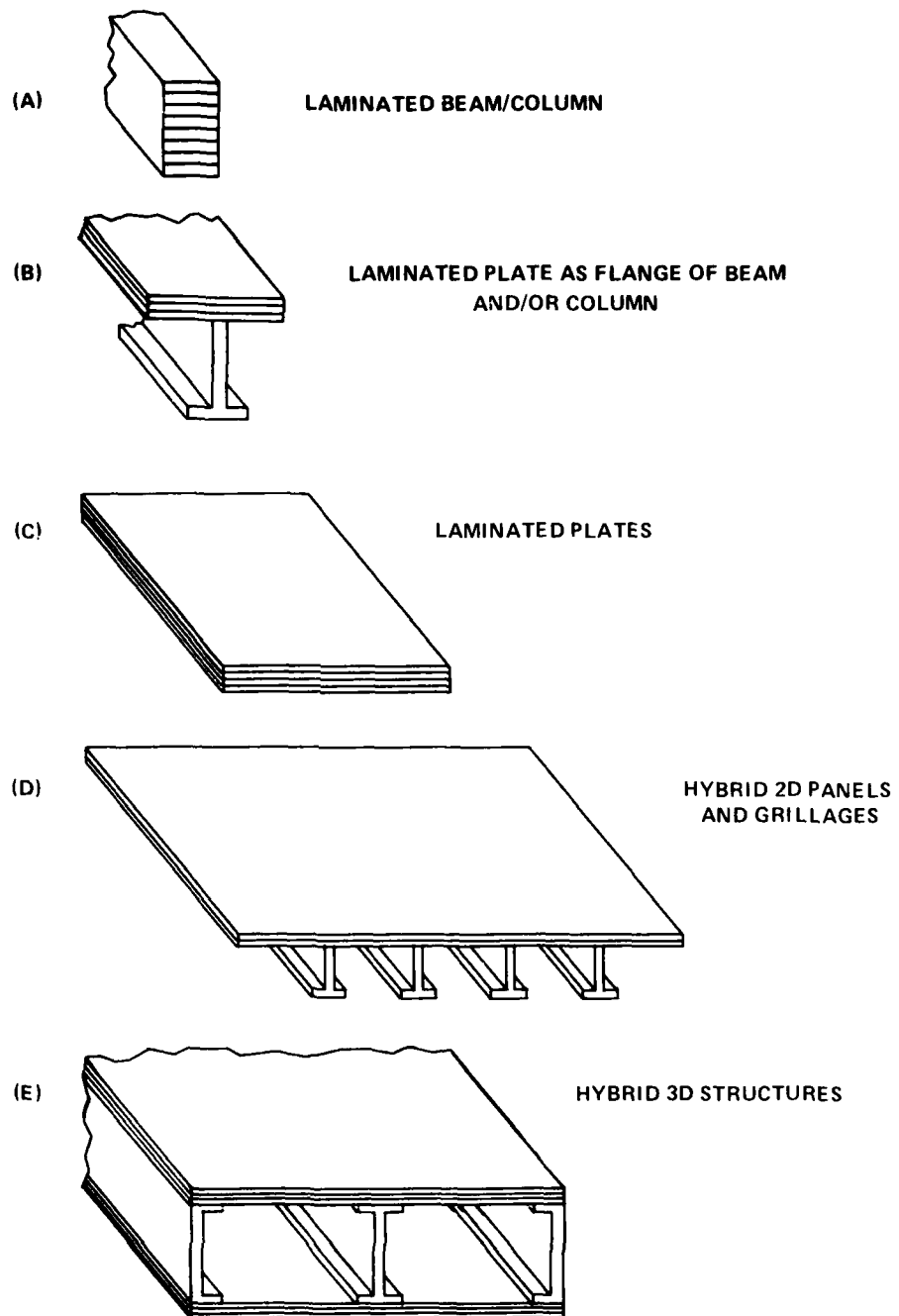
Figure 4 - Structural Applications for Laminated Composites

5

Numerous methods, carried over from the analysis of metallic structures, are available for analyzing laminated composites in the above applications. These methods include: strength-of-materials techniques and formulas; classical methods for the bending, buckling, and vibration of laminated plates; and the finite-element method for the analysis of more complex hybrid structures (see Table 1). The extension of these analysis methods from structures made of isotropic and homogeneous materials, for example, metallic, to ones involving laminated composites necessitates that the laminated composite materials be replaced by "equivalent" homogeneous anisotropic materials having the same stiffness properties during extensional and bending deformations (see Figure 5). The required analyses are then performed on the new structure where the laminated structural components are assumed to be made of this "equivalent" material.

LAMINATED AND EQUIVALENT (NONLAMINATED) BEAM OR COLUMN
COLUMN

(a)

NOTE: ABOVE PROPORTIONS FOR $E_f < E_w$

BEAM WITH LAMINATED FLANGES AND EQUIVALENT
MODELS

(b)
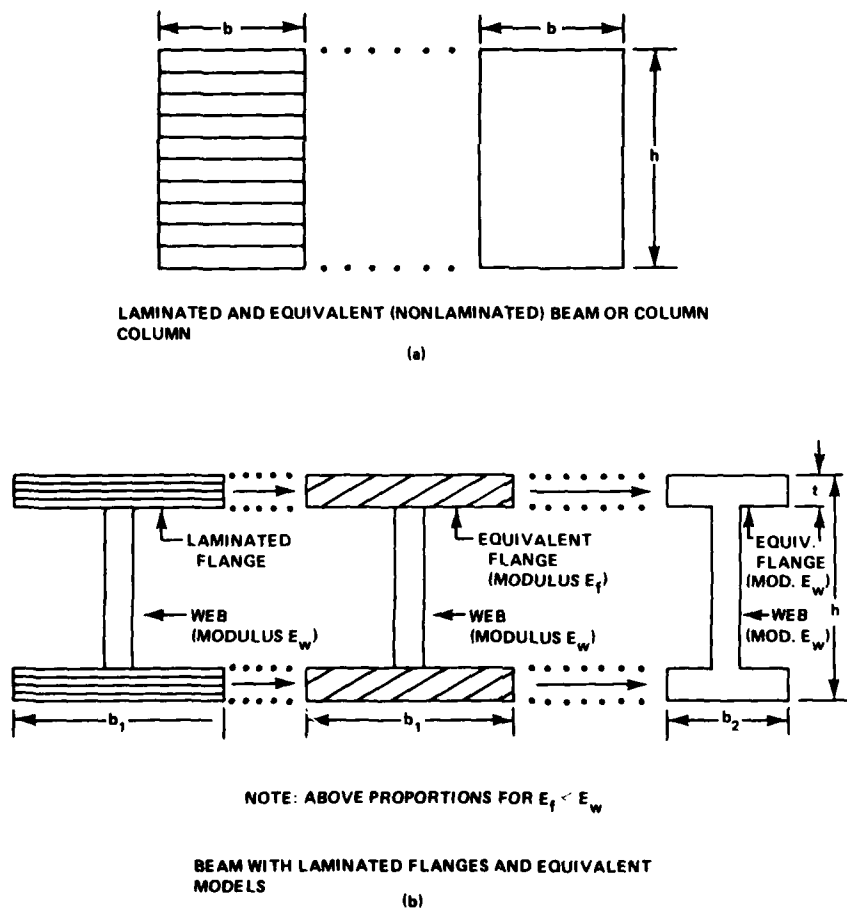
Figure 5 - Illustration of Modeling Procedures for Laminated Beams and Columns

6

The first part of this report will present procedures[3,4] for solving for the equivalent stiffness properties based on the principles of laminated plate theory.[5,6] The elastic properties needed in the structural analysis of laminates are of three kinds (Table 1):  (a) engineering constants for conventional strength-of-materials-type calculations, (b) extensional and bending stiffnesses for classical bending, buckling, and vibrational analyses of laminated plates, and (c) reduced stiffnesses for finite-element analyses of structural components involving laminates.  The necessity for three different representations of laminate stiffness, and the distinction between them, will be brought out later in the report.

The task of characterizing elastic properties of laminated composites may be performed analytically, experimentally, or both.  The use of laboratory component tests to establish the elastic properties of a laminate for many different lamina layups and fiber orientations is costly, so motivation exists for having an experimentally valid analytical tool with the same capability.  One of several available computer programs having this analytical capability is discussed later in the report. This and the other programs require as input data the unidirectional engineering constants (parallel and perpendicular to the fibers) of the individual layers or laminas which make up a laminate.  Although these unidirectional engineering constants may be determined analytically, it is common practice to experimentally measure the constants using coupon tests.

TABLE 1 - EQUIVALENT STIFFNESS PROPERTIES AND METHODS
OF ANALYSIS FOR LAMINATED COMPOSITES

| Methods of Analysis | Types of Stiffness Properties |
|---|---|
| Strength of Materials (Formulas, etc.) | Engineering Constants-- $E_x$, $E_y$, $\nu_{xy}$, $\nu_{yx}$, $G_{xy}$ |
| Classical Plate Solution | Extensional and Bending Stiffnesses-- $A_{ij}$, $B_{ij}$, $D_{ij}$ |
| Finite Element | Reduced Stiffnesses $Q^*_{ij}$<br>$Q^*_{ij(m)}$ -Membrane Response<br>$Q^*_{ij(b)}$ -Bending Response |

Following a discussion of the procedures for determining the elastic properties of laminates, the use of these properties in implementing the analytical methods referred to earlier will be discussed. In order to assess the effectiveness of the strength-of-material and finite-element methods for laminate applications, numerical and test results are reported and compared for a composite box beam simulating the forward foil of the PCH-1 hydrofoil.

## EQUIVALENT ELASTIC PROPERTIES OF LAMINATES

This section describes the computational procedures for determining the equivalent elastic properties of laminates which are needed in analyzing structures employing laminated composites. It will be seen that these various kinds of elastic properties are interrelated and are natural to the particular type of analysis being performed. Engineering constants are common to design and analysis methods based on strength-of-materials techniques; extensional and bending stiffnesses are natural to classical methods of analyses, including finite-difference techniques; reduced stiffnesses are used for finite-element analyses. Because the engineering constants and reduced stiffnesses may be derived from the extensional and bending stiffnesses, the latter are now discussed.

## EXTENSIONAL AND BENDING STIFFNESSES

Mathematical expressions for the extensional and bending stiffnesses of a laminate may be derived using the theory of laminated plates, or lamination theory as it is called.[5,6] This theory is employed to not only generate equivalent stiffness parameters for laminates, but also to form the basis for laminate stress analyses. Lamination theory is based on the following assumptions: (a) a perfect bond exists between the layers of a laminate (no slippage between layers); (b) the laminated plate is thin, i.e., thickness is small compared to the lateral dimensions of the plate; and (c) normals to the layers of a laminate remain perpendicular to the layers (shearing strains $\gamma_{xz} = \gamma_{yz} = 0$) and do not change length ($\varepsilon_z = 0$) during laminate bending. The coordinate system for defining $\varepsilon_z$, $\gamma_{xz}$, and $\gamma_{yz}$ has the z axis perpendicular to the laminate and the x and y axes lying in the plane of the laminate (see Figure 6). It should be noted that assumptions (b) and (c) above correspond to the Kirchoff theory for plates and the Kirchoff-Love theories for shells.

$$\begin{Bmatrix} N_x \\ N_y \\ N_{xy} \end{Bmatrix} = \begin{bmatrix} A_{11} & A_{12} & A_{16} \\ A_{12} & A_{22} & A_{26} \\ A_{16} & A_{26} & A_{66} \end{bmatrix} \begin{Bmatrix} \epsilon_x \\ \epsilon_y \\ \gamma_{xy} \end{Bmatrix}$$



$$\begin{Bmatrix} M_x \\ M_y \\ M_{xy} \end{Bmatrix} = \begin{bmatrix} D_{11} & D_{12} & D_{16} \\ D_{12} & D_{22} & D_{26} \\ D_{16} & D_{26} & D_{66} \end{bmatrix} \begin{Bmatrix} k_x \\ k_y \\ k_{xy} \end{Bmatrix}$$
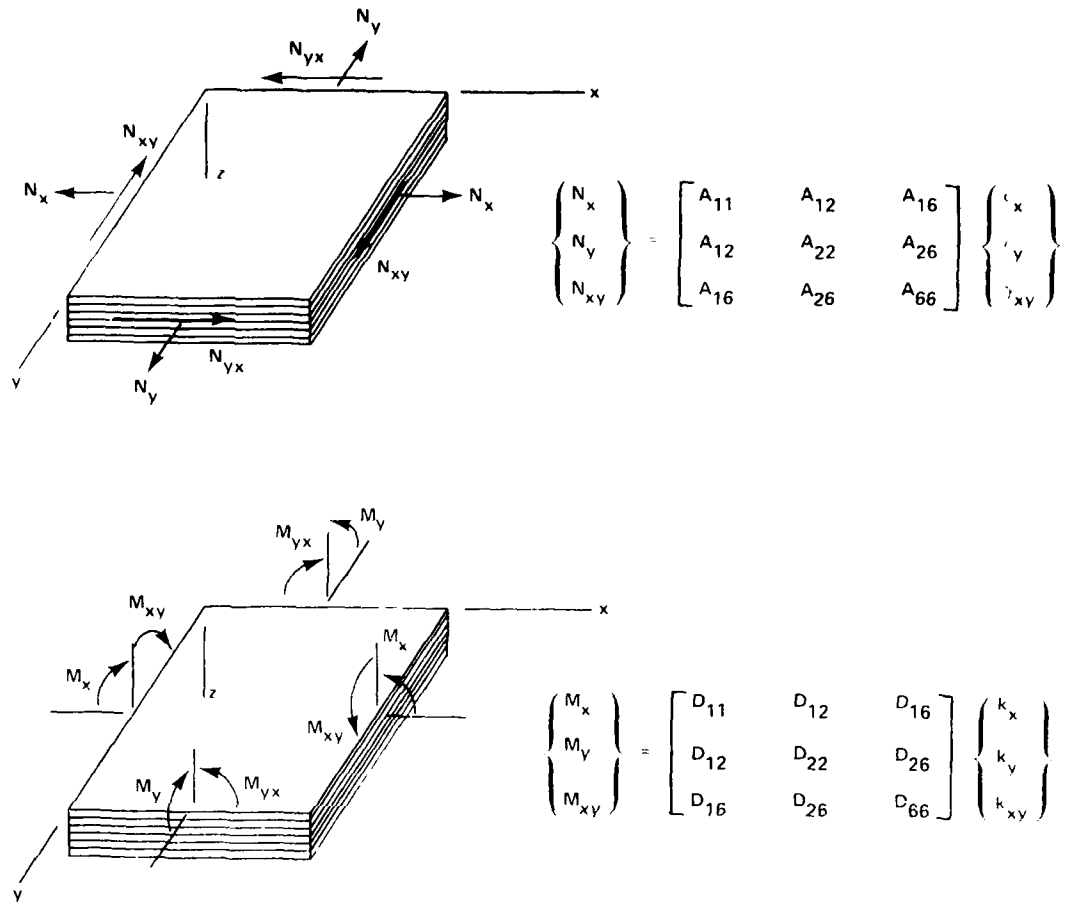
Figure 6 - Relationship between (a) In-Plane Forces and Strains and (b) Moments and Curvatures in Flat Symmetric Laminates

The extensional stiffnesses $A_{ij}$ of a laminate relate the in-plane forces $N_x$, $N_y$, and $N_{xy}$ per unit width to the in-plane strains $\epsilon_x$, $\epsilon_y$, and $\gamma_{xy}$ of the middle surface (see Figure 6a). Similarly, the bending stiffnesses $D_{ij}$ relate the out-of-plane bending moments $M_x$ and $M_y$ and twisting moments $M_{xy}$ per unit width to the resulting out-of-plane curvatures $k_x$, $k_y$, and $k_{xy}$ of the middle surface (see Figure 6b). In laminates where the layup of layers or laminas about the middle surface is not symmetric, either because of fiber orientation and/or material properties, a coupling between extension (including shear) and bending (including twisting) occurs. In other words, the application of in-plane forces not only produces

9

in-plane strains but also causes out-of-plane bending and associated curvatures. Likewise, any bending moments applied to the laminate will produce in-plane strains. The stiffness parameters which relate in-plane forces to out-of-plane curvatures and which relate moments to in-plane strains are referred to as coupling stiffnesses $B_{ij}$. Mathematically, these relationships are expressed in matrix form by

$$
\begin{Bmatrix} N_x \\ N_y \\ N_{xy} \\ \hline M_x \\ M_y \\ M_{xy} \end{Bmatrix} = \begin{bmatrix} A_{11} & A_{12} & A_{16} & B_{11} & B_{12} & B_{16} \\ A_{12} & A_{22} & A_{26} & B_{12} & B_{22} & B_{26} \\ A_{16} & A_{26} & A_{66} & B_{16} & B_{26} & B_{66} \\ \hline B_{11} & B_{12} & B_{16} & D_{11} & D_{12} & D_{16} \\ B_{12} & B_{22} & B_{26} & D_{12} & D_{22} & D_{26} \\ B_{16} & B_{26} & B_{66} & D_{16} & D_{26} & D_{66} \end{bmatrix} \begin{Bmatrix} \varepsilon_x \\ \varepsilon_y \\ \gamma_{xy} \\ \hline k_x \\ k_y \\ k_{xy} \end{Bmatrix}
\tag{1}
$$

or, in condensed form, by

$$
\begin{Bmatrix} \dfrac{N}{M} \end{Bmatrix} = \begin{bmatrix} \dfrac{A}{B} & \dfrac{B}{D} \end{bmatrix} \begin{Bmatrix} \dfrac{\varepsilon}{k} \end{Bmatrix}
\tag{2}
$$

The extensional, coupling, and bending stiffnesses respectively, $A_{ij}$, $B_{ij}$, and $D_{ij}$ in Equation (2) are expressed and determined as follows:

$$
A_{ij} = \int_{-h/2}^{h/2} \overline{Q}_{ij} \, dz = \sum_{k=1}^{N} (\overline{Q}_{ij})_k \, (z_k - z_{k-1})
$$

$$
B_{ij} = \int_{-h/2}^{h/2} \overline{Q}_{ij} \, z \, dz = \frac{1}{2} \sum_{k=1}^{N} (\overline{Q}_{ij})_k \, (z_k^2 - z_{k-1}^2)
\tag{3}
$$

$$
D_{ij} = \int_{-h/2}^{h/2} \overline{Q}_{ij} \, z^2 \, dz = \frac{1}{3} \sum_{k=1}^{N} (\overline{Q}_{ij})_k \, (z_k^3 - z_{k-1}^3)
$$

where the $\overline{Q}_{ij}$ parameters are referred to as reduced stiffnesses[5] and constitute the elements of the two-dimensional orthotropic stress-strain relations for the individual layers of a laminate. These stress-strain relations are given by

$$\left\{ \begin{array}{c} \sigma_x \\ \sigma_y \\ \tau_{xy} \end{array} \right\} = \left[ \begin{array}{ccc} \overline{Q}_{11} & \overline{Q}_{12} & \overline{Q}_{16} \\ \overline{Q}_{12} & \overline{Q}_{22} & \overline{Q}_{26} \\ \overline{Q}_{16} & \overline{Q}_{26} & \overline{Q}_{66} \end{array} \right] \left\{ \begin{array}{c} \varepsilon_x \\ \varepsilon_y \\ \gamma_{xy} \end{array} \right\} \tag{4}$$

which are defined with respect to the direction of the loads on the laminate. The appearance of the stiffness elements $\overline{Q}_{16}$, $\overline{Q}_{26}$, and $\overline{Q}_{66}$, instead of $\overline{Q}_{13}$, $\overline{Q}_{23}$, and $\overline{Q}_{33}$, follows from the fact that Equations (4) are obtained by reducing the $6 \times 6$ stress-strain matrix for 3-dimensional behavior (see Reference 5). Appendices A and B and Reference 5 discuss the detailed procedure for determining the extensional and bending stiffnesses $A_{ij}$ and $D_{ij}$ ($B_{ij}$ elements are zero because the laminate considered is symmetric). The basic steps involved are summarized as follows:

1. Determine the reduced stiffness $Q_{ij}$ for each of the laminas (see Appendix A, Section A.1) using available unidirectional elastic moduli $E_1$, $E_2$, $\nu_{12}$, $\nu_{21}$, and $G_{12}$ for each of the laminas.

2. Transform these $Q_{ij}$, defined with respect to the so-called material directions (parallel and normal to the fibers), to the directions of the laminate axes* x and y, resulting in $\overline{Q}_{ij}$ (see Appendix A, Section A.2).

3. Substitute the $\overline{Q}_{ij}$ into Equations (3) and solve for the $A_{ij}$ and $D_{ij}$ (see Appendix B).

The steps just outlined can be straightforwardly, but tediously, used to compute the required stiffnesses $A_{ij}$, $B_{ij}$, and $D_{ij}$ for any given laminate. The calculation procedure is demonstrated in Appendix C for a graphite-epoxy laminated skin (symmetric with $B_{ij} = 0$) of the composite box beam in Figure 1.

At this point, it is worthwhile discussing the effect of such laminate characteristics as symmetry, fiber orientation, etc., on the magnitudes of the stiffness coefficients $A_{ij}$, $B_{ij}$, and $D_{ij}$ in Equation (2). Laminates for which the A, B, and D

*The x and y directions for a laminate are usually chosen as follows for a laminated beam and column: x along the member and y normal to the member in the plane of the laminate; for a laminated plate: x and y are parallel to the long and short sides of plate, respectively; for laminates which are components of 2D and 3D hybrid structures: any conveniently oriented x and y axes (z too) may be used.

matrices in Equation (2) are completely full (i.e., no zero elements) represent the most general case encountered (nonsymmetric laminates with multiple anisotropic layers). In practice, a structural designer frequently tries to avoid this general laminate case in order to (a) minimize analytical complexity, (b) eliminate modes of deformation which could adversely affect the load capacity of the laminated member (e.g., out-of-plane bending and/or twisting deformations associated with the coupling stiffnesses $B_{ij}$ will reduce the load capacity of a laminated plate under in-plane loads), and (c) prevent twisting of laminates when subject to temperature changes and in-plane boundary restraint. Instead, the designer often tries to select or buildup a laminate having symmetry about the midplane so that the coupling coefficients $B_{ij}$ in Equation (2) are all equal to zero. Figure 7 shows how this is achieved for cross-ply and angle-ply laminates. Note that symmetry requires that the laminate layers, which are shown reflected (as in a mirror) about the middle plane, must have the same thickness, elastic properties, and angles of orientation relative to the x and y axes.

Beyond the simplification in Equations (2) due to symmetry ($B_{ij} = 0$), simplifications in the A and D matrices also occur if additional conditions are imposed on the arrangement of layers within the laminate. Figure 7 indicates two classes of symmetric laminates which may be somewhat easily discussed: the symmetric cross-ply and the symmetric angle-ply laminate.

For the case of symmetric cross-ply laminates, whether thay are regular (e.g., 90°, 0°, 90°) or irregular* (e.g., 90°, 0°, 0°, 90°) in layup, the coupling coefficients $A_{16}$, $A_{26}$, $D_{16}$, and $D_{26}$ are all equal to zero. Coupling coefficients $A_{16}$ and $A_{26}$ relate extensional forces $N_x$ and $N_y$ to shear strain $\gamma_{xy}$ (and shear force $N_{xy}$ to extensional strains $\varepsilon_x$ and $\varepsilon_y$). Similarly, coupling coefficients $D_{16}$ and $D_{26}$ relate bending moments $M_x$ and $M_y$ to twisting curvature $k_{xy}$, and twisting moment $M_{xy}$ to bending curvatures $k_x$ and $k_y$. The zeroing out of $A_{16}$, $A_{26}$, $D_{16}$, and $D_{26}$ for symmetric cross-ply laminates follows directly from the fact that the reduced stiffnesses $\overline{Q}_{16}$ and $\overline{Q}_{26}$ are zero for all of the layers of the cross-ply laminate.

Turning next to the symmetric angle-ply laminates in Figure 7, the picture is more complicated. For the regular angle-ply laminates (e.g., $+\alpha$, $-\alpha$, $+\alpha$), the $A_{16}$, $A_{26}$, $D_{16}$, and $D_{26}$ take on small (nonzero) values. However, for the irregular*

---

*Irregular here denotes laminates where the orientations of successive layers do not simply alternate signs or directions as in regular laminates.

12

**EXAMPLE—REGULAR (90˚, 0˚, 90˚)**
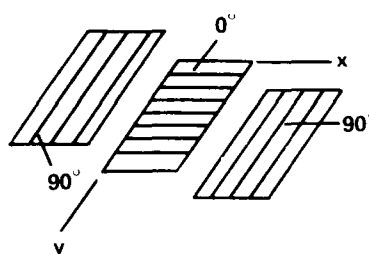
**COUPLING COEFFICIENTS**

$B_{ij}$    0 (DUE TO SYMMETRY)

$A_{16}$    $A_{26}$ = 0

$D_{16}$    $D_{26}$ = 0

FOR <u>REGULAR</u> OR <u>IRREGULAR</u>
CASES (ANY NUMBER OF LAYERS)

**EXAMPLE—REGULAR (+α, α, +α)**
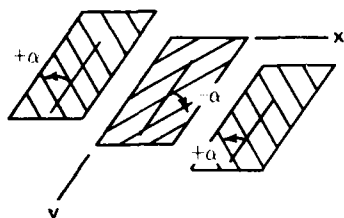
**OTHER EXAMPLES**

(R)  +α,   α,   +α
(I)′ +α,  −α,   α,   +α
(R)  +α,   α,  +α,   α,   +α
(I)  +α,   α,  +α,  +α,   α,   +α
(R)  +α,   α,  +α,   α,  +α,   α,  +α,
(I)′ +α,   α,  +α,   α,  −α,  +α,   α,  +α

**COUPLING COEFFICIENTS**

$B_{ij}$ = 0 (DUE TO SYMMETRY)

<u>REGULAR LAYUPS</u>
$A_{16}, A_{26}, D_{16}, D_{26}$ ──►TAKE ON SMALL
                          VALUES──►(R) ABOVE

<u>IRREGULAR LAYUPS</u>
$A_{16}, A_{26}, D_{16}, D_{26}$ ──►TAKE ON SMALL
                          VALUES──►(I) ABOVE
$A_{16}, A_{26}, D_{16}, D_{26}$ = 0   (I)′ ABOVE

Figure 7 – Coupling Coefficients for (a) Symmetric Cross-Ply (Specially
Orthotropic) and (b) Symmetric Angle-Ply Laminates

symmetric angle-ply laminates, the coupling coefficients may either be zero or non-
zero in value depending upon the laminate layup arrangement (orientations of the
successive layers) as pointed out in Figure 7. Lastly, it should be noted that a
symmetric laminate put together from a combination of cross-plys and angle-plys may
also be shown to lead to zero on nonzero values for the coupling coefficients depend-
ing on the arrangement of layers within the laminate.

Recall for the regular symmetric angle-ply laminates, that the coupling coeffi-cients $A_{16}$, $A_{26}$, $D_{16}$, and $D_{26}$ took on small nonzero values. In these instances the analyst should be cautioned to not set the off-diagonal terms equal to zero simply because they happen to be small. An indication of the effect of setting the off-diagonal terms $D_{16}$ and $D_{26}$ equal to zero, i.e., treating the angle-ply laminated plate as specially orthotropic, is provided by two examples from Jones.[5] The first example is a uniformly loaded square plate for which $D_{22}/D_{11} = 1$, $(D_{12} + 2D_{66})/D_{11} = 1.5$, and $D_{16}/D_{11} = D_{26}/D_{11} = -0.5$. For this problem, setting the twist coupling coefficients $D_{16}$ and $D_{26}$ equal to zero results in calculated plate deflections which are 24 percent less than the analytical predictions where these coefficients have not been set equal to zero. The second example in Jones[5] has to do with the buckling of a rectangular laminated plate made up of twenty boron-epoxy layers having alternating + and − angles of orientation with respect to the overall plate axes. It is pointed out for this example in Jones that the specially orthotropic approximation leads to an overestimate of the plate buckling load. Additional angle-ply laminates need to be looked at before it can be determined just how small the $D_{16}$ and $D_{26}$ have to be before they can be safely set equal to zero in laminate deflection and buckling analyses.

ENGINEERING CONSTANTS

At the preliminary design stage, many aspects of structural behavior for lami-nated composite members (Figure 1) may be initially evaluated using strength-of-materials techniques once the necessary engineering constants for the laminates are available. These engineering constants may be calculated from the extensional stiffnesses $A_{ij}$ after their values have been determined using the procedure described previously and found in Appendices A and B. Methods will be discussed below for calculating the following engineering constants for laminated composites:

$E_x$ and $E_y$ — Young's moduli
$\nu_{xy}$ and $\nu_{yx}$ — Poisson's ratios
$G_{xy}$ — Shear modulus
$\eta_{x,xy}$ and $\eta_{y,xy}$ — Coefficients of mutual influence of the first kind
$\eta_{xy,x}$ and $\eta_{xy,y}$ — Coefficients of mutual influence of the second kind

14

The first three types of engineering constants above, i.e., Young's modulus, Poisson's ratio, and shear modulus, are already familiar to those individuals involved with the design and analysis of metallic structures. The "coefficients of mutual influence," however, are most probably not familiar. Therefore, stated simply, the coefficients of mutual influence of the first kind relate a normal strain in the x direction to a shearing strain in the xy plane ($\eta_{x,xy}$) or relate a normal strain in the y direction to a shearing strain in the xy plane ($\eta_{y,xy}$). Similarly, the coefficients of mutual influence of the second kind relate a shearing strain in the xy plane to a normal strain in the x direction ($\eta_{xy,x}$) or to a normal strain in the y direction ($\eta_{xy,y}$). As an example, $\eta_{xy,x}$ is expressed by

$$\eta_{xy,x} = \gamma_{xy}/\varepsilon_x$$

where $\gamma_{xy}$ is the shearing strain in the xy plane associated with a normal strain in the x direction $\varepsilon_x$ (usually produced by a normal stress $\sigma_x$).

Methods of Calculation

Several computational procedures may be used to establish the engineering constants for laminated composite materials. One procedure, not discussed here, is contained in a paper by Greszczuk.[3] A second procedure, given in a paper by Smith,[4] is probably more suitable for computer implementation than the first and is described below.

Under in-plane load conditions, the in-plane forces on the laminated components in structural applications (a) through (e) of Figure 4 are related to the in-plane strains by

$$N_x = A_{11} \varepsilon_x + A_{12} \varepsilon_y + A_{16} \gamma_{xy}$$
$$N_y = A_{12} \varepsilon_x + A_{22} \varepsilon_y + A_{26} \gamma_{xy} \quad (5)$$
$$N_{xy} = A_{16} \varepsilon_x + A_{26} \varepsilon_y + A_{66} \gamma_{xy}$$

or, in matrix form, by

15

$$\{N\} = [A] \{\varepsilon\}$$

Solving for $\{\varepsilon\}$ in terms of $\{N\}$ we have $\{\varepsilon\} = [A]^{-1} \{N\} = [\bar{A}] \{N\}$, or written out,

$$\varepsilon_x = \bar{A}_{11} N_x + \bar{A}_{12} N_y + \bar{A}_{16} N_{xy}$$

$$\varepsilon_y = \bar{A}_{12} N_x + \bar{A}_{22} N_y + \bar{A}_{26} N_{xy} \qquad (6)$$

$$\gamma_{xy} = \bar{A}_{16} N_x + \bar{A}_{26} N_y + \bar{A}_{66} N_{xy}$$

where the $\bar{A}_{ij}$ are the elements of the matrix $[\bar{A}]$ which is the inverse of $[A]$. The $\bar{A}_{ij}$ are found from

$$\bar{A}_{11} = (A_{22} A_{66} - A_{26}^2)/\Delta$$

$$\bar{A}_{12} = -(A_{12} A_{66} - A_{16} A_{26})/\Delta$$

$$\bar{A}_{22} = (A_{11} A_{66} - A_{16}^2)/\Delta$$

$$\bar{A}_{16} = (A_{12} A_{26} - A_{16} A_{22})/\Delta \qquad (7)$$

$$\bar{A}_{26} = -(A_{11} A_{26} - A_{16} A_{12})/\Delta$$

$$\bar{A}_{66} = (A_{11} A_{22} - A_{12}^2)/\Delta$$

where

$$\Delta = A_{11}(A_{22} A_{66} - A_{26}^2) - A_{12}(A_{12} A_{66} - A_{16} A_{26})$$

$$+ A_{16}(A_{12} A_{26} - A_{16} A_{22})$$

Once the $\bar{A}_{ij}$ above are known, these quantities may be used to compute the engineering constants. Expressions relating the engineering constants and the $\bar{A}_{ij}$ are obtained using Equation (6). The procedure for deriving expressions for $E_x$ and $\eta_{xy,x}$ is now shown. (Similar procedures may be used to derive expressions for the other engineering constants.)

<u>Deriving $E_x$.</u>

Setting $N_y = N_{xy} = 0$ in the first of Equations (6), we have

$$\epsilon_x = \overline{A}_{11} \, N_x$$

But,

$$\epsilon_x = \sigma_x/E_x = (N_x/h)/E_x$$

Therefore, equating both expressions for $\epsilon_x$ above and then solving for $E_x$,

$$E_x = 1/(\overline{A}_{11} h) \tag{8}$$

where h is the full thickness of the laminate.


<u>Deriving $\eta_{xy,x}$.</u>

Setting $N_y = N_{xy} = 0$ in the third of Equations (6),

$$\gamma_{xy} = \overline{A}_{16} \, N_x$$

Substituting $N_x = \sigma_x h = E_x \, \epsilon_x h$ into the above equation,

$$\gamma_{xy} = \overline{A}_{16} \, E_x \, \epsilon_x h$$

Now, as defined earlier,

$$\eta_{xy,x} = \gamma_{xy}/\epsilon_x$$

so,

$$\eta_{xy,x} = \frac{\overline{A}_{16} \, E_x \, \epsilon_x h}{\epsilon_x} = \overline{A}_{16} \, E_x \, h$$

Therefore, after substituting Equation (8) above for $E_x$,

$$\eta_{xy,x} = \overline{A}_{16}/\overline{A}_{11}$$

Having shown the procedures for deriving two of the engineering constants, the final expressions for all of the engineering constants (including those just derived) are now summarized:

$$E_x = 1/(\overline{A}_{11}h)$$

$$E_y = 1/(\overline{A}_{22}h)$$

$$\nu_{xy} = -\varepsilon_y/\varepsilon_x = -\overline{A}_{12}/\overline{A}_{11}$$

$$\nu_{yx} = -\varepsilon_x/\varepsilon_y = -\overline{A}_{12}/\overline{A}_{22}$$

$$G_{xy} = 1/(\overline{A}_{66}h) \qquad\qquad (9)$$

$$\eta_{xy,x} = \overline{A}_{16}/\overline{A}_{11} \,^{*}$$

$$\eta_{xy,y} = \overline{A}_{26}/\overline{A}_{22} \,^{*}$$

$$\eta_{x,xy} = \overline{A}_{16}/\overline{A}_{66}$$

$$\eta_{y,xy} = \overline{A}_{26}/\overline{A}_{66}$$

A simplification of the process for calculating engineering constants is possible for the regular symmetric cross-ply laminates in Figure 7.

For this case, since $A_{16} = A_{26} = 0$, we have, using Equations (7) and (9),

$$\Delta = A_{11}\,A_{22}\,A_{66} - A_{12}^{2}\,A_{66}$$

and

$$\overline{A}_{11} = (A_{22}\,A_{66} - A_{26}^{2})/\Delta = A_{22}\,A_{66}/(A_{11}\,A_{22}\,A_{66} - A_{12}^{2}\,A_{66})$$

Therefore,

$$E_x = 1/(\overline{A}_{11}h) = (A_{11} - A_{12}^{2}/A_{22})/h \qquad\qquad (10)$$

---

*References 4 and 5 only included expressions for the coefficients of the second kind $\eta_{xy,x}$ and $\eta_{xy,y}$. It would appear that these coefficients are more frequently used than the coefficients of the first kind $\eta_{x,xy}$ and $\eta_{y,xy}$.

Similarly, it may be shown that

$$E_y = (A_{22} - A_{12}^2/A_{11})/h$$

$$\nu_{xy} = A_{12}/A_{22}$$

$$\nu_{yx} = A_{12}/A_{11} \tag{11}$$

$$G_{xy} = A_{66}/h$$

and

$$\eta_{xy,x} = \eta_{xy,y} = \eta_{x,xy} = \eta_{y,xy} = 0$$

It should again be emphasized that these formulas only apply for regular symmetric cross-ply and not angle-ply laminas. For angle ply, Equations (8) and (9) in terms of $\overline{A}_{ij}$ must be used.

## Experimental Verification

Using the two methods of calculation referred to in the previous section, engineering constants have been determined for a laminated composite consisting of 53 plies of T300 graphite fibers oriented 0° to the loading direction and 32 plies of GY70 graphite fibers oriented $\pm45°$. Based on Method I (Smith's paper[4]), engineering constants are calculated in Appendix C and are reported in the first column of Table 2. Engineering constants based on Method II (Greszczuk's work[3]) were taken from the theoretical curves of Reference 1 (reproduced in Figures 8-12) by reading off the data points for a T300 and GY70 hybrid composition of 55.3 percent and 44.7 percent, respectively. The theoretically predicted engineering constants in Table 2 are seen to be in close agreement with the experimentally measured values[1] for the hybrid laminate. It is concluded that either Method I or II is sufficiently accurate for calculating the engineering constants for composit laminates under in-plane force and strain conditions. Since both methods are mathematically equivalent, the very slight difference in numerical values is most probably associated with (a) interpolating the theoretical values from the theoretical curves in Figures 8-12 for specified percentages of T300 and GY70 and (b) plotting up the theoretical curves in Figures 8-12 in the first place.

TABLE 2 - COMPARISON OF THEORETICAL AND EXPERIMENTAL STIFFNESS
PROPERTIES FOR BOX BEAM HYBRID COMPOSITE
(THORNEL T300 AND CELION GY70)

| Engineering Constant | Theoretical (Method I)[4] | Theoretical (Method II)[3] | Experimental[3] |
|---|---|---|---|
| $E_x$ | 12.67 | 12.6 | 13.04 |
| $E_y$ | 4.64 | 4.6 | 4.17 |
| $\nu_{xy}$ | 0.804 | 0.800 | 0.766 |
| $\nu_{yx}$ | 0.294 | 0.295 | 0.244 |
| $G_{xy}$ | 5.26 | 5.2 | 5.09 |

## COMPUTER PROGRAM

Since the procedure for the calculation of extensional, bending, and coupling stiffnesses, as well as the engineering constant, is a rather tedious one, especially for a composite laminate involving many layers, computer programs have been written to automate the process. One such program[7] is called SQ5 and is available through the Aerospace Structures Information and Analysis Center, Wright-Patterson Air Force Base, Ohio. This program calculates the laminate stiffness properties mentioned above and performs a stress analysis for a given set of applied in-plane forces and moments.

The theoretical basis for SQ5 is plate lamination theory.[5,6] First, for a given laminate, the elements of matrix Equation (1) are generated. These equations are then solved for the in-plane strains and curvatures in terms of applied forces and moments by inverting the A and D matrices ($B_{ij} = 0$). The strains and curvatures are next used to determine the strains and stresses in each lamina. Temperature-induced stress and m ment resultants may also be calculated and then added to the other known loads. The thermal analysis assumes a constant temperature throughout the laminate thickness. The program also includes a simplified transverse shear

Figure 8 – Young's Modules $E_x$ of Laminate as Function of Percent of GY70 (+45 Degrees) and T300 (0 Degree, 90 Degrees) Material (from Reference 1)

21

Figure 9 - Young's Modulus $E_y$ of Laminate as Function of Percent of GY70 (±45 Degrees) and T300 (0 Degree, 90 Degrees) Material (from Reference 1)

22
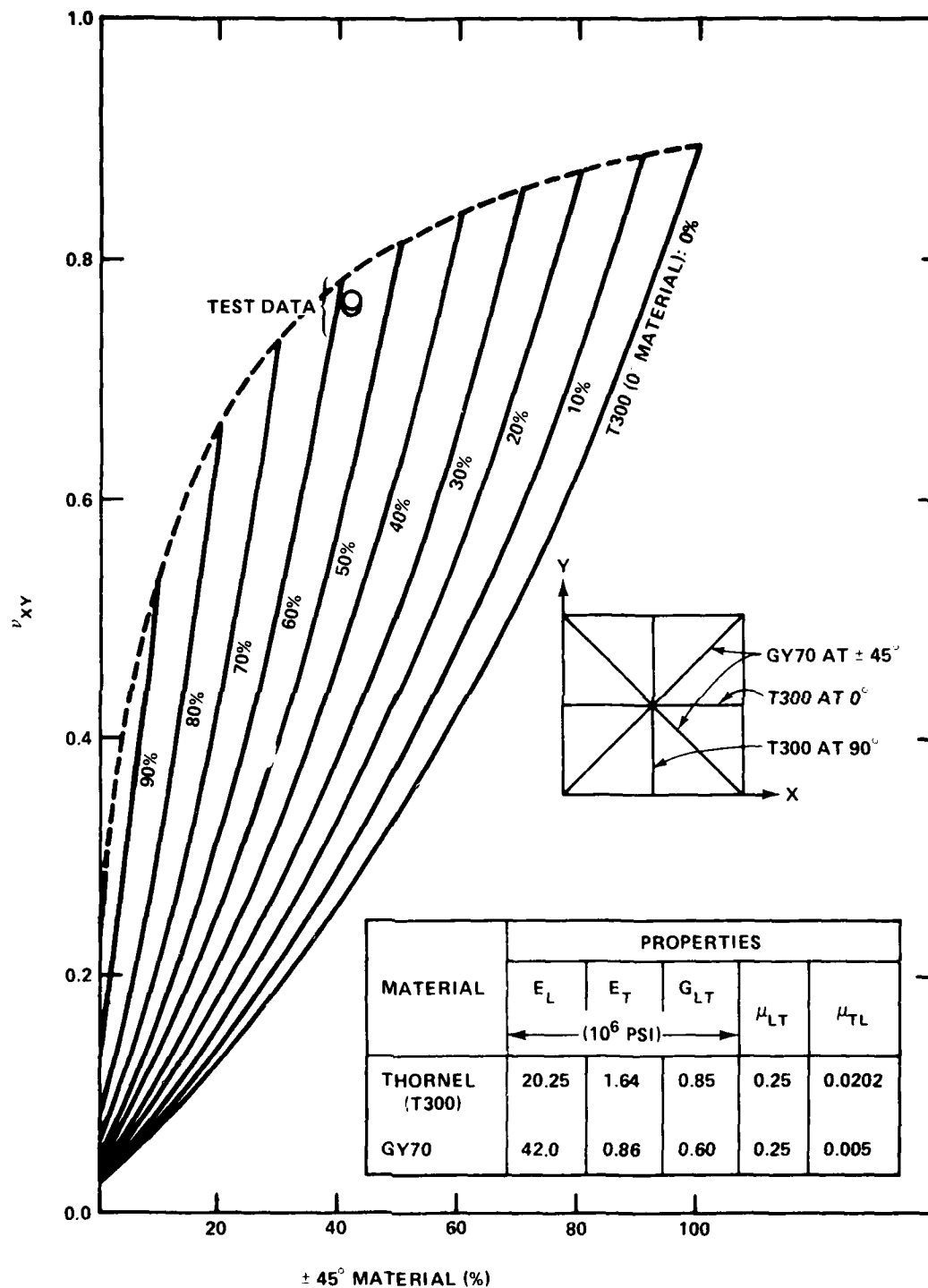
Figure 10 - Poisson's Ratio $\nu_{xy}$ of Laminate as Function of Percent of GY70 ($\pm$45 Degrees) and T300 (0 Degree, 90 Degrees) Material (from Reference 1)
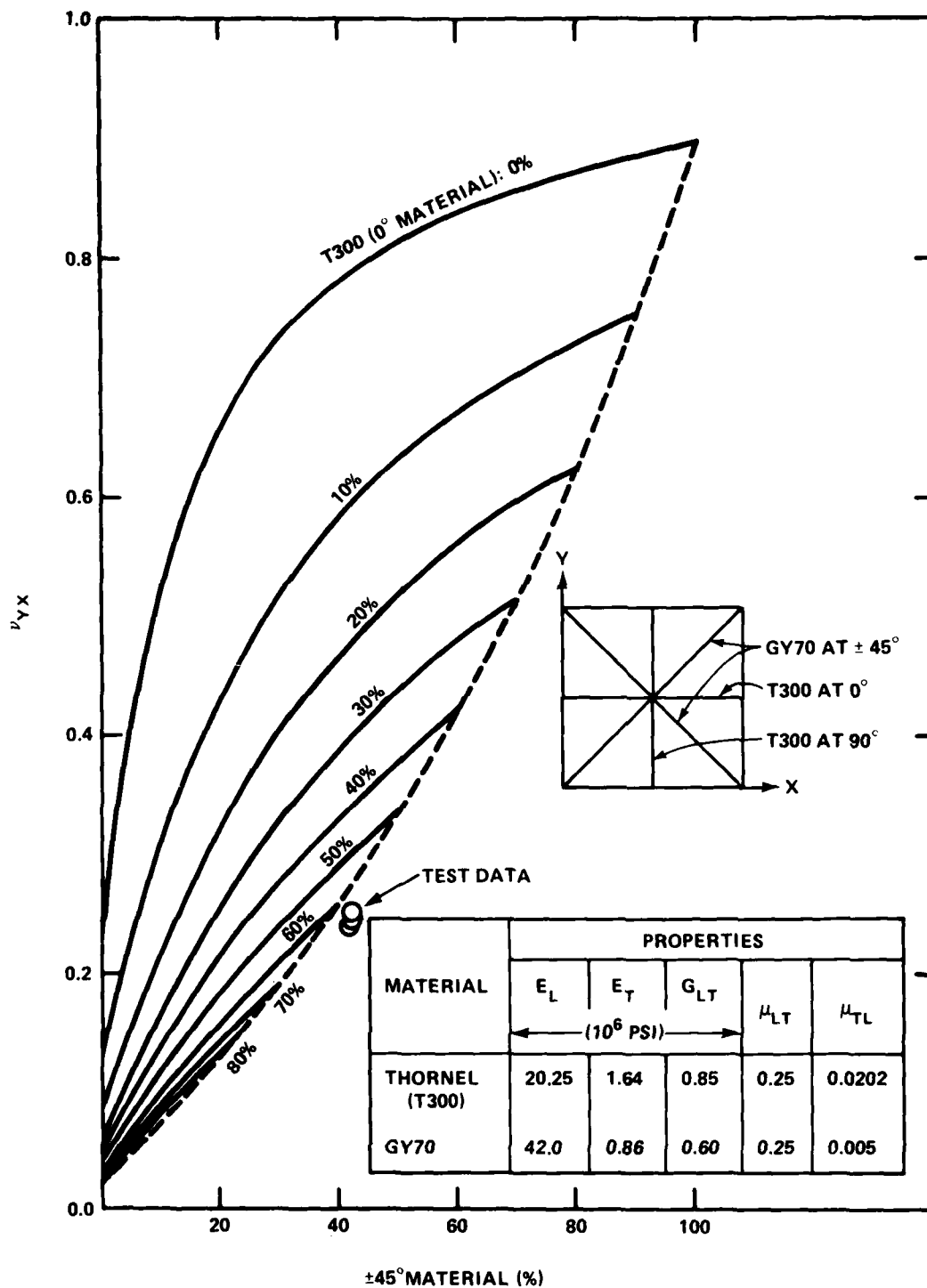
Figure 11 - Poisson's Ratio $\nu_{yx}$ of Laminate as Function of Percent of GY70 (±45 Degrees) and T300 (0 Degree, 90 Degrees) Material (from Reference 1)

24

PROPERTIES

| MATERIAL | $E_L$ | $E_T$ | $G_{LT}$ | $\mu_{LT}$ | $\mu_{TL}$ |
|---|---|---|---|---|---|
| | ← | $(10^6$ PSI) | → | | |
| THORNEL (T300) | 20.25 | 1.64 | 0.85 | 0.25 | 0.0202 |
| GY70 | 42.0 | 0.86 | 0.60 | 0.25 | 0.005 |

TEST DATA

$G_{XY}$ ($10^6$ PSI)
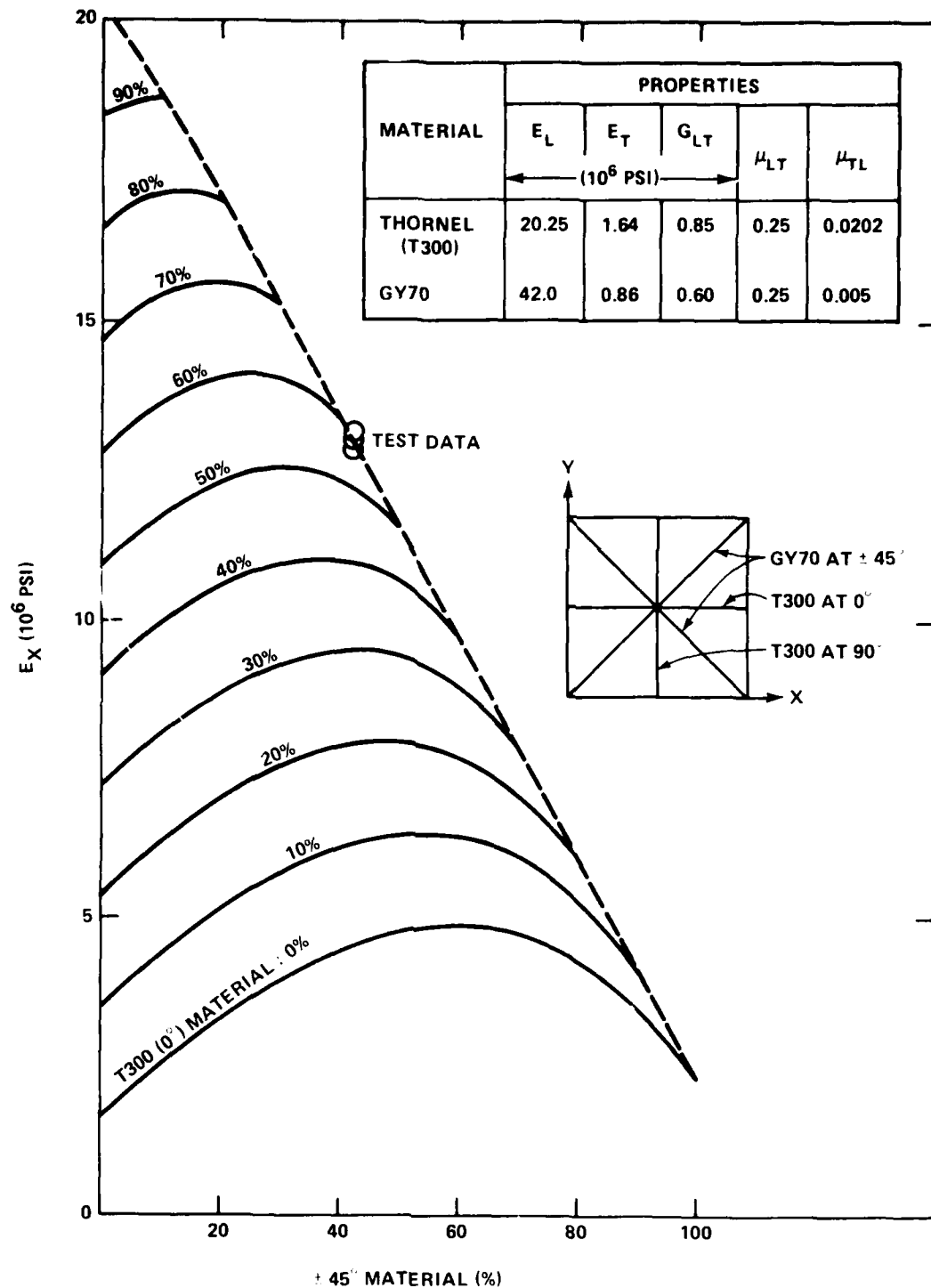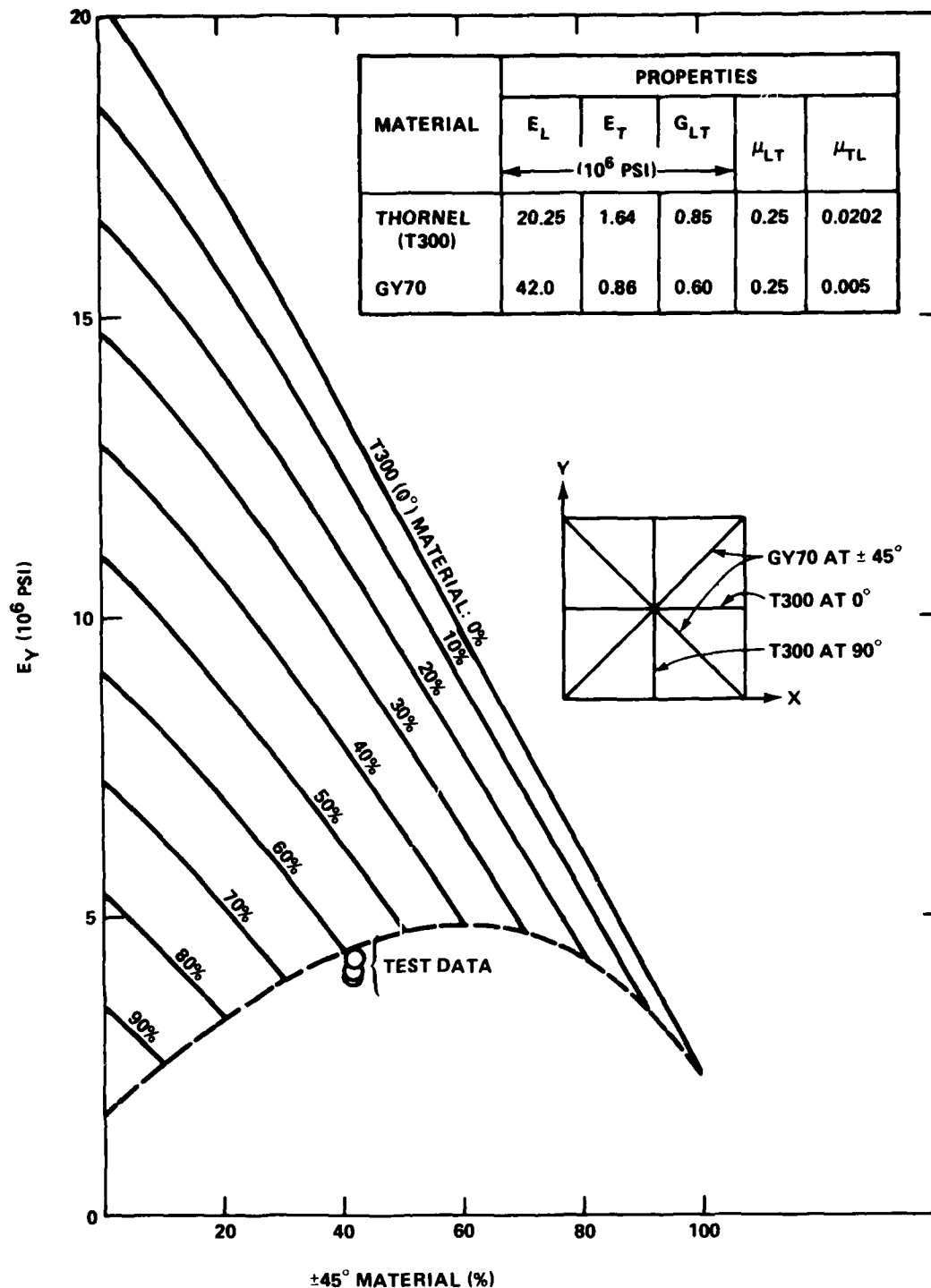
GY70 AT ± 45

T300 AT 0

T300 AT 90
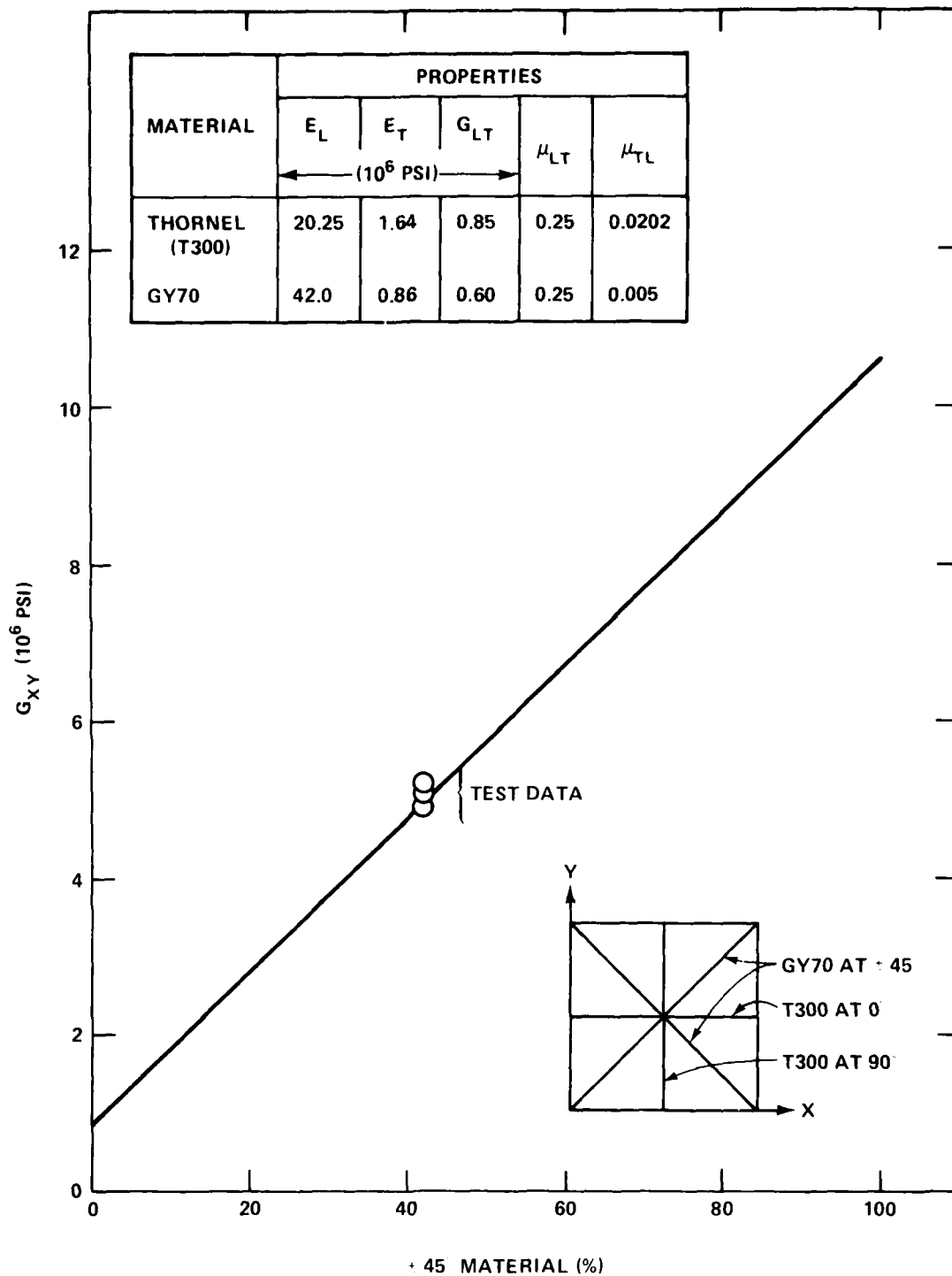
· 45 MATERIAL (%)

Figure 12 – Shear Modulus $G_{xy}$ of Laminate as Function of Percent of GY70 (±45 Degrees) and T300 (0 Degree, 90 Degrees) Material (from Reference 1)

25

analysis in which the shear stress distribution across the laminate thickness due to known shear resultants $Q_x$ and $Q_y$ is predicted. It also has the capability to obtain a laminate interaction diagram based upon the maximum strain theory of failure. A description of the input data needed to use the program SQ5, excerpted from Reference 7, is provided in Appendix D.

# ANALYSIS OF LAMINATES

## STRENGTH-OF-MATERIALS METHODS

Strength-of-materials methods and formulas are useful in varying degrees for all of the structural applications of Table 1 once the appropriate equivalent elastic properties for the laminate have been found. However, these methods are probably most effective for structural applications (a) and (b) in Figure 4 which are concerned with laminated beams and columns. In application (a), the cross section of the member is considered to be laminated from top to bottom and has a rectangular cross section (see Figure 5). In application (b), only the flange or flanges of the member are of laminated construction (Figure 5). The web consists of a homogeneous and isotropic metallic or nonmetallic material.

## Laminated Beams and Columns

In fabricating beams or columns, it is advantageous to stack the layers so as to provide symmetry about the midplane and, thereby, eliminate coupling between extensional and bending responses, as discussed earlier. All layers should probably be oriented with the fibers parallel to the length of the beam. In some engineering situations, a laminated member may not be fabricated from scratch but may be obtained simply by cutting a narrow strip from a laminated plate which is readily available and may have been laid up for other purposes. In these cases, the orientation of fibers in the individual layers of the laminate may be oriented in either a cross-ply or angle-ply arrangement, or a combination of both.

26

The governing differential equation for the deflection of a laminated beam or plate strip* (Figure 4a) is given by

$$E_b I \frac{d^2 y}{dx^2} = M_x \tag{12}$$

where y is beam deflection, $M_x$ is bending moment, $E_b$ is the engineering constant for an equivalent beam having the same bending rigidity $E_b I$ as the actual laminated beam (see Figure 5a), and I is cross-sectional moment of inertia (the equivalent beam is assumed to have the same cross-sectional dimensions, and therefore moment of inertia I, as the laminated beam).

In order to obtain beam deflections by integrating Equation (12) and satisfying boundary conditions, the engineering constant $E_b$ for the equivalent beam must be determined. To do this, one starts with the moment-curvature relations, in inverted form, for a laminated plate

$$k_x = \overline{D}_{11} M_x + \overline{D}_{12} M_y + \overline{D}_{16} M_{xy}$$

$$k_y = \overline{D}_{12} M_x + \overline{D}_{22} M_y + \overline{D}_{26} M_{xy} \tag{13}$$

$$k_{xy} = \overline{D}_{16} M_x + \overline{D}_{26} M_y + \overline{D}_{66} M_{xy}$$

which are analogous to Equations (6) involving in-plane forces and strains. Setting $M_y = M_{xy} = 0$ in the first of Equations (13), to represent one-dimensional (beam) bending,

$$k_x = \overline{D}_{11} M_x$$

or

$$\frac{1}{\overline{D}_{11}} k_x = M_x \tag{14}$$

---

*The plate strip here is assumed to be in a state of plane stress. If it is desired to model the plate strip as an element of an entire plate, it is necessary to assume a plane-strain condition for the sides of the strip and to start with the appropriate differential equation.

which applies for a beam or strip of unit width. For a beam of width b, we have

$$\frac{b}{\overline{D}_{11}} \frac{d^2 y}{dx^2} = M_x \tag{15}$$

Comparing Equations (15) and (12), we see that the equivalent engineering constant $E_b$ is obtained from

$$E_b I = b/\overline{D}_{11} \qquad \left( I = \frac{1}{12} bh^3 \right)$$

or

$$E_b \left( \frac{1}{12} bh^3 \right) = \frac{b}{\overline{D}_{11}}$$

from which

$$E_b = 12/(\overline{D}_{11} h^3) \tag{16}$$

It should be noted here that $E_b$ associated with the bending response of a laminate is different from $E_x$ in Equation (8) associated with the extensional response. This relates to the fact that $E_b$ is dependent upon the stacking sequence, but $E_x$ is not.

The bending stiffness $\overline{D}_{11}$ in Equation (16) is needed to solve for $E_b$. The stiffness $\overline{D}_{11}$ is given by

$$\overline{D}_{11} = (D_{22} D_{66} - D_{26}^2)/\Delta$$

where

$$\Delta = D_{11}(D_{22} D_{66} - D_{26}^2) - D_{12}(D_{12} D_{66} - D_{16} D_{26})$$

$$+ D_{16}(D_{12} D_{26} - D_{16} D_{22})$$

28

For regular symmetric cross-ply laminates (Figure 7), $D_{16} = D_{26} = 0$.
Therefore,

$$\bar{D}_{11} = \frac{1}{D_{11} - D_{12}^2/D_{22}}$$

and

$$E_b = \frac{12 \ (D_{11} - D_{12}^2/D_{22})}{h^3} \tag{17}$$

In addition to determining deflections of a laminated beam using Equations (12) and (16), interest also exists in determining stresses. A coarse estimate of stress in the laminated beam is obtained from the formula

$$\sigma_x = \frac{M_x c}{I} \tag{18}$$

where M is the bending moment, c is the distance from the neutral surface to the fiber location, and I is the beam cross-sectional inertia.

A more accurate estimate of stress in any particular layer of the beam may be obtained as follows. Using Equation (18), the longitudinal strain in any layer of the beam is obtained from

$$\varepsilon_x = \sigma_x/E_b = \frac{M_x c}{E_b I} \tag{19}$$

The lateral strain in the beam is found using

$$\varepsilon_y = - \nu_{xy} \ \varepsilon_x \tag{20}$$

where $\nu_{xy}$ is given by one of Equations (9) for a laminate under extension.* Then, the stress in any layer is given by

---

*We are neglecting the fact that the laminate is really under bending and not extension in obtaining $\nu_{xy}$. In order to be more consistent, $E_b$ in Equation (19) could be replaced by $E_x$ from Equation (8).

$$\sigma_x = \overline{Q}_{11} \, \epsilon_x + \overline{Q}_{12} \, \epsilon_y$$

$$\sigma_y = \overline{Q}_{12} \, \epsilon_x + \overline{Q}_{22} \, \epsilon_y \qquad (21)$$

where the reduced stiffnesses $\overline{Q}_{11}$, $\overline{Q}_{12}$, and $\overline{Q}_{22}$ are found for any layer or lamina of the beam using the theory and procedures given in the first two sections of Appendix A. The stress $\sigma_x$ will probably dominate over $\sigma_y$.

Equation (16) for $E_b$ is also needed for determining the buckling load of a laminated column or plate strip. The critical buckling load is given by the Euler formula

$$P_{cr} = \pi^2 E_b I / L^2 \qquad (22)$$

for a pinned-end laminated column of length L and cross-sectional moment of inertia I.*

Members with Laminated Flanges

It is anticipated that laminated members may involve, in some instances, a homogeneous metallic web with a laminated flange as illustrated in Figure 5b. In addition to the I beam shown, the hybrid structural member may also take the form of a T beam. An approximate determination of the flexural rigidity $E_b I$ for these hybrid members may be accomplished using a two-step process as shown in Figure 5b. In the first step, the hybrid I-member with laminated flanges is converted into a hybrid I-member with homogeneous flanges by mathematically replacing the laminated flange material with a nonlaminated material having an equivalent engineering constant $E_f$. The equivalent constant $E_f$ is found using Equations (7) and (8) given earlier. The second step is to convert the hybrid member with a homogeneous flange material to a nonhybrid member where the flange material is replaced by a new flange of width $b_2$, having a modulus $E_w$ identical to that of the web of the I beam. The new required flange with $b_2$ is found from

$$b_2 = \frac{E_f b_1}{E_w}$$

_____

*See a strength-of-material text or handbook for dealing with other end boundary conditions.

30

Once the initial hybrid beam has been converted into the final equivalent beam just described, the moment of inertia $I_2$ is computed for this final cross section. The flexural rigidity $E_w I_2$ is then substituted for $E_b I$ in Equation (12) for calculating beam deflections and in Equations (19) as the first step in determining stresses in the individual layers of the laminated flange. Finally, it should be pointed out that the analysis procedure for a structural member with a laminated flange introduces an approximation which is not present in the laminated beam analysis of Figure 5a. The approximation is associated with computing the equivalent flange modulus $E_f$ above by assuming that the strain distribution over the depth of the flange is uniform. Actually, the strain distribution varies slightly due to bending of the overall beam cross section.

CLASSICAL METHODS

Laminated plating has potential applications in panels, grillages, and three-dimensional hybrid structures, as illustrated in Figure 4. For analysis purposes, the plating in these applications may often be modeled as a single plate, as shown in Figure 13, if appropriate edge boundary conditions are selected.

Timoshenko[8] and Jones[5] discuss classical methods for analyzing the bending, buckling, and vibration of rectangular orthotropic plates which may be directly applied to regular symmetric cross-ply laminates (see Figure 7). One of the approximate solution techniques described in these references uses Fourier series to represent the plate loading and deflection shape. Formulas are presented in the next section which were derived based on this approach. As mentioned above, the formulas apply to specially orthotropic laminates involving cross-ply fibers for which the stiffnesses $D_{16}$ and $D_{26}$ in Equations (1)-(3) are equal to zero. The solution procedure for regular symmetric angle-ply laminates is more complex since the $D_{16}$ and $D_{26}$ stiffnesses are no longer zero but may be small when a large number of layers are involved. The analysis of nonsymmetric laminas involving nonzero $B_{ij}$ coupling stiffnesses between extension and bending introduces even further complexity into the analysis.
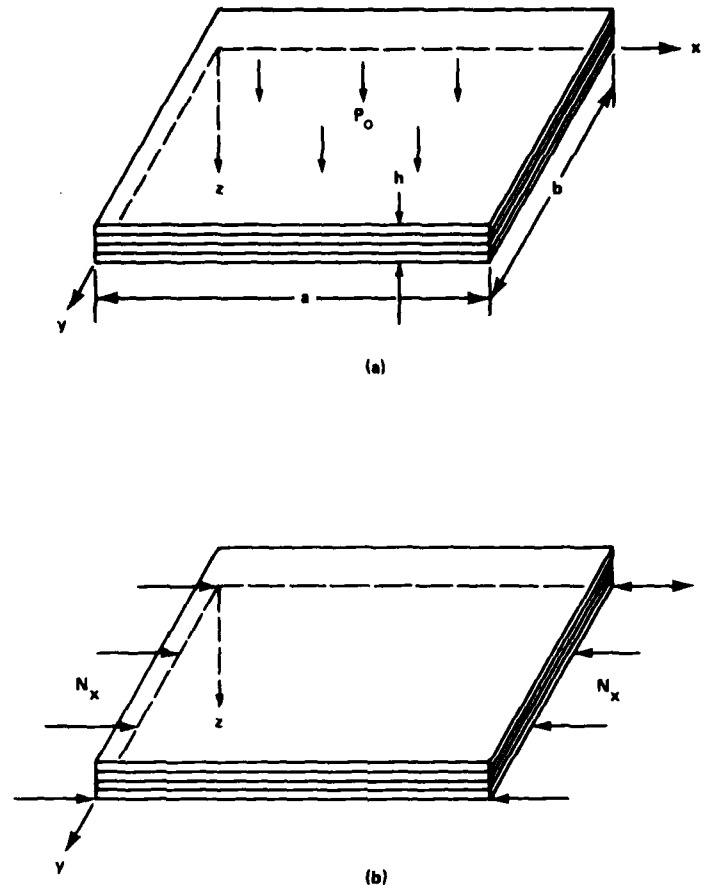
Figure 13 - Simply Supported Laminated Plates Subjected to (a) Lateral
Bending and (b) Buckling Under In-Plane Loads

Lateral Bending of Laminated Plates

Using the solution procedure of Navier which is described by Timoshenko[8] and
Jones,[5] the deflection of a uniformly loaded plate with simply supported edges is
given by

$$w(x,y) = \frac{16p_0}{\pi^6} \sum_{m=1,3,5,\ldots} \sum_{n=1,3,5,\ldots} \frac{\frac{1}{mn} \sin\left(\frac{m\pi x}{a}\right) \sin\left(\frac{n\pi y}{b}\right)}{D_{11}\left(\frac{m}{a}\right)^4 + 2\left(D_{12} + 2D_{66}\right)\left(\frac{m}{a}\right)^2 \left(\frac{n}{b}\right)^2 + D_{22}\left(\frac{n}{b}\right)^4}$$

(23)

where $p_0$ is the uniform load per unit area,

a and b are the side dimensions of the plate,

x and y are variable distances parallel to a and b sides of plate,

m and n are odd integers, and

$D_{11}$, $D_{12}$, $D_{22}$ and $D_{66}$ are defined in Equation (3) and computed in Appendix B for a given example of a four-layer laminate.

The strains in any layer of the laminate at a distance z from the middle surface may be found by substituting Equation (23) for w into

$$\varepsilon_x = - z \frac{\partial^2 w}{\partial x^2}$$

$$\varepsilon_y = - z \frac{\partial^2 w}{\partial y^2}$$

(24)

and

$$\gamma_{xy} = - z \frac{\partial^2 w}{\partial x \partial y}$$

Stresses are then obtained by substituting Equations (24) for strain into Equations (4). By following the procedure just outlined, formulas have been generated for computing these stresses. In arriving at these formulas, the series in Equation (23) has been written out for m taking on values of 1 and 3 and for n taking on values of 1 and 3. The stresses in any layer are then given by

$$\sigma_x = \overline{Q}_{11} \, \varepsilon_x + \overline{Q}_{12} \, \varepsilon_y$$

and

$$\sigma_y = \overline{Q}_{12} \, \varepsilon_x + \overline{Q}_{22} \, \varepsilon_y$$

(25)

where

$$\varepsilon_x = \frac{16 p_0 z}{\pi^6} \{(C_1 + C_2)(\pi/a)^2 + (C_3 + C_4)(3\pi/a)^2\}$$

and

$$\varepsilon_y = \frac{16 p_0 z}{\pi^6} \{(C_1 + C_3)(\pi/b)^2 + (C_2 + C_4)(3\pi/b)^2\}$$

33

and

$$C_1 = 1/\{D_{11}(1/a)^4 + 2(D_{12}+D_{66})(1/a)^2(1/b)^2 + D_{22}(1/b)^4\}$$

$$C_2 = (-1/3)/\{D_{11}(1/a)^4 + 2(D_{12}+D_{66})(1/a)^2(3/b)^2 + D_{22}(3/b)^4\}$$

$$C_3 = (-1/3)/\{D_{11}(3/a)^4 + 2(D_{12}+D_{66})(3/a)^2(1/b)^2 + D_{22}(1/b)^4\}$$

$$C_4 = (1/9)/\{D_{11}(3/a)^4 + 2(D_{12}+D_{66})(3/a)^2(3/b)^2 + D_{22}(3/b)^4\}$$

The stiffnesses $\overline{Q}_{11}$, $\overline{Q}_{12}$, and $\overline{Q}_{22}$ are calculated for each layer using equations in Appendix A.


Buckling and Vibration

Equations are presented in this section for calculating the buckling loads and vibration frequencies of rectangular laminated plates having simply supported boundaries and a regular symmetric cross-ply layup of fibers (defined as specially orthotropic plate, see Figure 7).

The buckling stress $\sigma_{cr}$ of a specially orthotropic plate under an axial loading (Figure 13) is given by[5,8,9]

$$\sigma_{cr} = \frac{\pi^2}{h}\left[D_{11}\left(\frac{m}{a}\right)^2 + 2(D_{12}+D_{66})\left(\frac{n}{b}\right)^2 + D_{22}\left(\frac{n}{b}\right)^4\left(\frac{a}{m}\right)^2\right] \tag{26}$$

where a, b, and h are the length, width, and thickness of the plate, m and n are integers indicating the number of buckle half wavelengths in the x and y directions, and $D_{11}$, $D_{12}$, and $D_{22}$ and $D_{66}$ are defined by Equations (1)-(3). Rearranging Equation (26) and recognizing that the lowest value of buckling stress will be associated with n = 1,

$$\sigma_{cr} = \left[D_{11}\left(\frac{mb}{a}\right)^2 + 2(D_{12}+2D_{66}) + D_{22}\left(\frac{a}{mb}\right)^2\right]\frac{\pi^2}{b^2 h} \tag{27}$$

The number m of half waves in the x direction is determined by taking the derivative $d\sigma_{cr}/dm$, setting it equal to zero, and solving for m. This gives

$$m = \frac{a}{b} \sqrt[4]{D_{22}/D_{11}} \qquad (28)$$

If the m computed using Equation (28) happens to be an integer, which is unlikely, this value of m gives the _actual_ number of half waves in the x direction, and the corresponding minimum buckling stress results from substituting Equation (28) into Equation (29), which gives

$$(\sigma_{cr})_{min} = [\sqrt{D_{11}\,D_{22}} + (D_{12}+2D_{66})] \frac{2\pi^2}{b^2 h} \qquad (29)$$

However, if the m computed from Equation (28) is not an integer—the most frequent case—it is necessary to substitute the next higher and lower integer values into Equation (27) to see which corresponds to the lower buckling stress. For example, if m is computed to be 1.6, one should try m = 1 and m = 2 in Equation (26) to see which m values results in the lower buckling stress. If m should turn out to be less than 1, say m = 0.6, then m = 1 corresponds to the lowest buckling mode and the corresponding critical stress is found by substituting m = 1 into Equation (27).

Buckling loads for specially orthotropic plates under other loading conditions (biaxial and shear) as well as other boundary conditions (such as two edges ly supported and two edges clamped or elastically restrained, or other combinations) are provided in Reference 9.

In addition to having analytical means for investigating the stability of laminated plates, tools are also needed to estimate the fundamental frequencies of vibration of laminated plates. Fundamental plate frequencies are necessary to insure that these frequencies are sufficiently removed from exciting frequencies due to machinery or other cyclic driving sources so as to prevent resonance or near-resonance conditions which may result in excessive deflections, fatigue, or other structural damage. The natural frequencies of vibration $\omega$ of rectangular laminated plates with simply supported boundaries may readily be computed using the equation

$$\omega^2 = \frac{\pi^4}{\rho} \left\{ D_{11} \left(\frac{m}{a}\right)^4 + 2(D_{12}+2D_{66}) \left(\frac{m}{a}\right)^2 \left(\frac{n}{b}\right)^2 + D_{22} \left(\frac{n}{b}\right)^4 \right\}$$

where $\rho$ is the mass density of the plate, a, b, and $D_{ij}$'s are identical to those defined for laterally loaded plates and buckling, and m and n refer to the different mode shapes of vibration. The fundamental frequency of vibration is obtained by setting m and n equal to 1. Reference 6 gives formulas for computing the natural frequencies of vibration for specially orthotropic laminated plates with all clamped boundaries or for various combinations of simply supported and clamped.

FINITE-ELEMENT METHODS

Analytical methods were given in the previous sections for analyzing several basic laminated components in hybrid structures. These methods isolate a laminated beam, column, or plate component of the structure and introduce the appropriate boundary and loading conditions to represent the interaction of the isolated member with the remainder of the structure. Since the results of these methods (strength-of-materials and classical analyses) are usually of an approximate nature, the methods are most suitable for application in the early stages of design. In order to obtain more accurate results in the later and final stages of design, the analyst frequently turns to the finite-element method and the computer programs which implement this method. One of the advantages of finite-element analyses is that these analyses minimize the number of assumptions as to the loading and constraints on the various components of the structure.

In analyzing hybrid structures, at least four options are available for modeling and treating the laminated components of the structure. These four approaches are illustrated in Figure 14 for the tapered composite box beam of Figure 1 which simulates the forward foil on the PCH-1 hydrofoil. The composite box beam has graphite epoxy laminated skins with internal steel spars and is supported and loaded as indicated in Figure 1.

Approach (1) in Figure 14 entails modeling the full laminated skin thickness in the box beam by equivalent two-dimensional (2D) plate elements having anisotropic material properties which are equivalent to those of the multilayered laminate.

36

(1) TWO-DIMENSIONAL FINITE
    ELEMENTS (xy PLANE) PROVIDE
    ● IN–PLANE STRESSES ($\sigma_x$, $\sigma_y$ AND $\tau_{xy}$)

(2) THREE-DIMENSIONAL FINITE
    ELEMENTS PROVIDE
    ● IN–PLANE STRESSES ($\sigma_x$, $\sigma_y$, $\tau_{xy}$)
    ● INTERLAMINAR AND NORMAL
      STRESSES ($\tau_{xz}$, $\tau_{yz}$, $\sigma_z$)

(3) TWO-DIMENSIONAL FINITE
    ELEMENTS (yz PLANE) PROVIDE
    ● IN–PLANE STRESSES ($\sigma_y$, $\sigma_x = 0$)
    ● INTERLAMINAR AND NORMAL
      STRESSES ($\tau_{zy}$ AND $\sigma_z$)

(4) THREE-DIMENSIONAL FINITE
    ELEMENTS PROVIDE
    ● IN–PLANE STRESSES ($\sigma_y$ AND $\sigma_x$)
    ● INTERLAMINAR AND NORMAL
      STRESSES ($\tau_{zy}$, $\tau_{zx}$, AND $\sigma_z$)

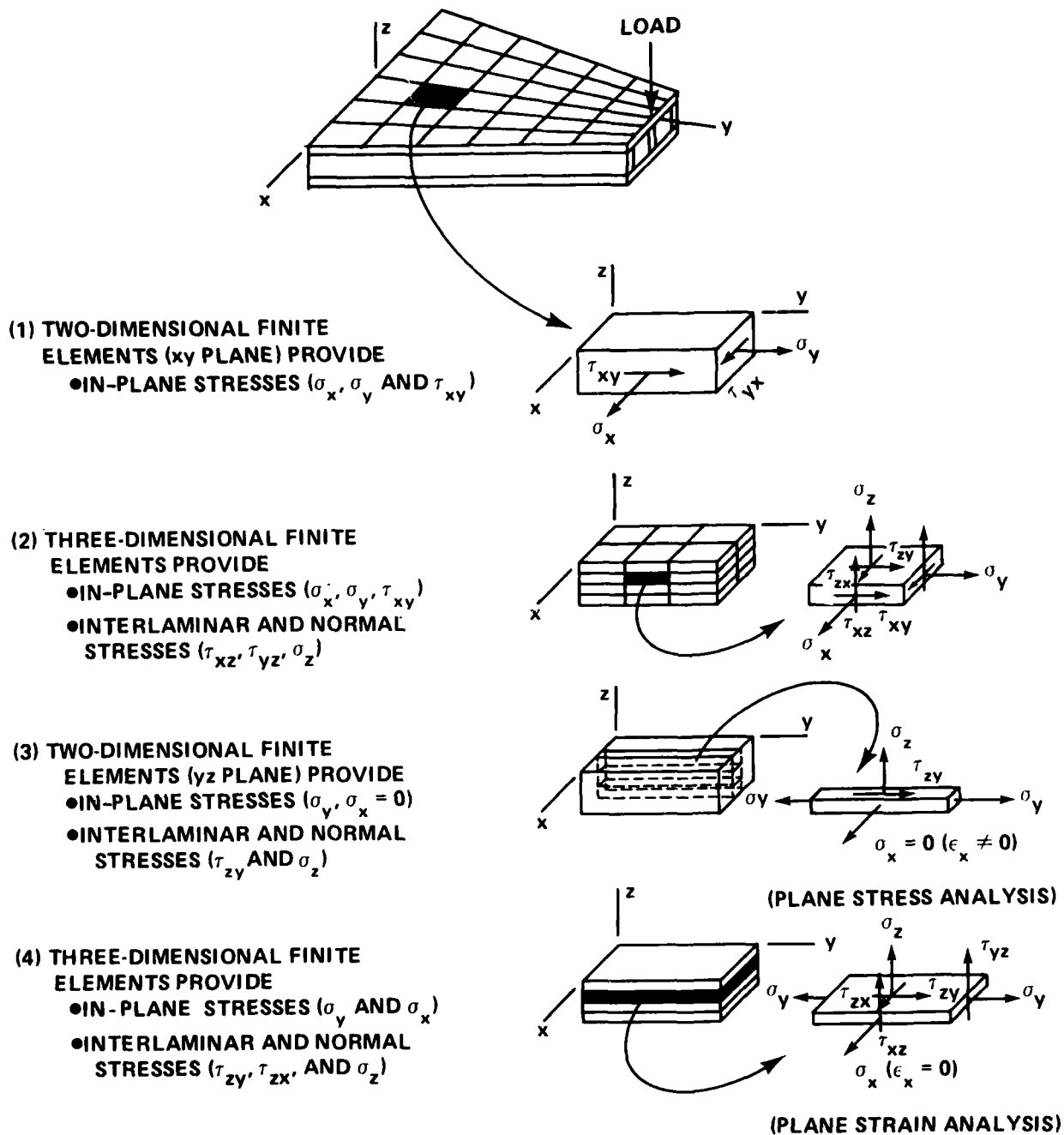(PLANE STRESS ANALYSIS)

(PLANE STRAIN ANALYSIS)

Figure 14 – Finite-Element Approaches for Laminated Skins in
Composite Box Beam

37

This modeling procedure was employed at DTNSRDC* in analyzing the composite box beam. The procedure allows a determination of the in-plane normal stresses $\sigma_x$ and $\sigma_y$ and shear stress $\tau_{xy}$ in the laminate, in an average or equivalent sense. These equivalent laminate stresses may be used to determine the in-plane stresses in the individual layers of the laminate in an approximate way (see Appendix F). However, it is not possible to determine the interlaminar shear stresses $\tau_{xz}$ and $\tau_{yz}$ by adopting equivalent 2D plate elements for the full laminate. The latter stresses are frequently the governing ones, particularly near free edges in laminates produced by cutting or drilling holes during fabrication.

Approaches (2) through (4) in Figure 14 facilitate a determination of interlaminar shear and normal stresses. In applying approach (2) in Figure 14, the laminate thickness is discretized by stacking a suitable number of 3-dimensional (3D) solid elements to represent the full thickness of the laminate. It is clearly not practical to have as many 3D elements vertically through the thickness as there are actual layers since there are frequently a large number of layers involved (approximately 80 layers for the skin of the box beam). Instead, the layers, may be grouped into as many layers as necessary (four layers in Figure 14) to determine the interlaminar shear and normal stresses at desired locations between layer or plies of the laminate. This second modeling approach was adopted by the Virginia Polytechnic Institute[10] (VPI) in analyzing the composite box beam. However, using this approach, the overall box beam deflection results were in agreement with neither the results of DTNSRDC's finite-element analyses using approach (1) nor with the box beam test results. It is suspected that the major reason that VPI's analysis did not agree with the others was their use of finite elements having very large aspect ratios. In addition, the distribution of interlaminar shear and normal stresses along the length of the box beam also exhibited some questionable oscillations. Therefore, further work is apparently still needed on the implementation of this approach.

Approaches (3) and (4) in Figure 14 utilize a beam-type model of the box beam. Because of this modeling approximation, the resulting interlaminar shear and normal stresses are not as accurate as they would be with approach (2) assuming all analyses are carried out properly. By stacking 2D-type elements in the yz plane in approach (3), a plane stress analysis is accomplished for which $\sigma_x = 0$, as indicated in

---

*Stein, M.C., "A Nastran Analysis of a Composite Laminate Box Beam for Application to Navy Hydrofoils," reported informally as enclosure (1) to DTNSRDC ltr 77-173-186 of 9 Dec 1977.

Figure 14. Since the box beam skins are, to some degree, restrained in the transverse direction by the load block at the one end and the clamping support at the other, a plane strain analysis where the transverse strains in the skin are set equal to zero (but $\sigma_x$ is not zero) may be a better approximation to the box behavior when using a beam-type model. This plane strain analysis may be accomplished by stacking 3D finite elements as indicated in approach (4) of Figure 14. It should be noted that in implementing approaches (3) and (4), it is important that the portion of the total box beam load which is carried by the beam strip be approximately determined and applied to the beam model. It also should be noted that both approaches (2) and (4), involving 3D elements, necessitate that five additional engineering constants (over those required with the 2D finite elements in approaches (1) and (3)) must be experimentally measured: $E_z$, $\nu_{xz}$, $\nu_{yz}$, $G_{xz}$, and $G_{yz}$. Finally, in terms of the cost to carry out the above approaches, it can be said that approach (3) will be the least costly and (2) the most costly. Approaches (1) and (4) will be somewhere in between in cost; it is difficult to rank them with respect to each other since the cost would be dependent on the number of elements used in each case.

Composite Box Beam Analysis

Using the computer program NASTRAN,[11] a finite-element analysis was performed by DTNSRDC on the composite box beam in Figure 1 to verify the results of a strength-of-materials analysis and to provide a more detailed insight into the beams structural behavior. The NASTRAN idealization for the box beam is shown in Figure 15. This report focuses on those aspects of the finite-element idealization and analysis concerned with the laminated skins since the steel spars may be modeled using procedures already familiar to the average NASTRAN user.

Modeling of Laminated Skin. The skin of the box beam is a reinforced epoxy laminate consisting of 44.6% GY70 at $\pm45°$ and 55.4% of T300 at $0°$, with a constant thickness of 0.5 in., except for regions near the load block and fixed end. The modeling of the laminated skin was accomplished using the NASTRAN plate element CQUAD1. According to the NASTRAN user's manual,[11] the CQUAD1 element is intended for application to sandwich plates having different elastic properties in bending, membrane, and shear. No mention is made of using CQUAD1 elements for laminated plates in the manual. However, the idea occurred at the beginning of the composite box beam

39

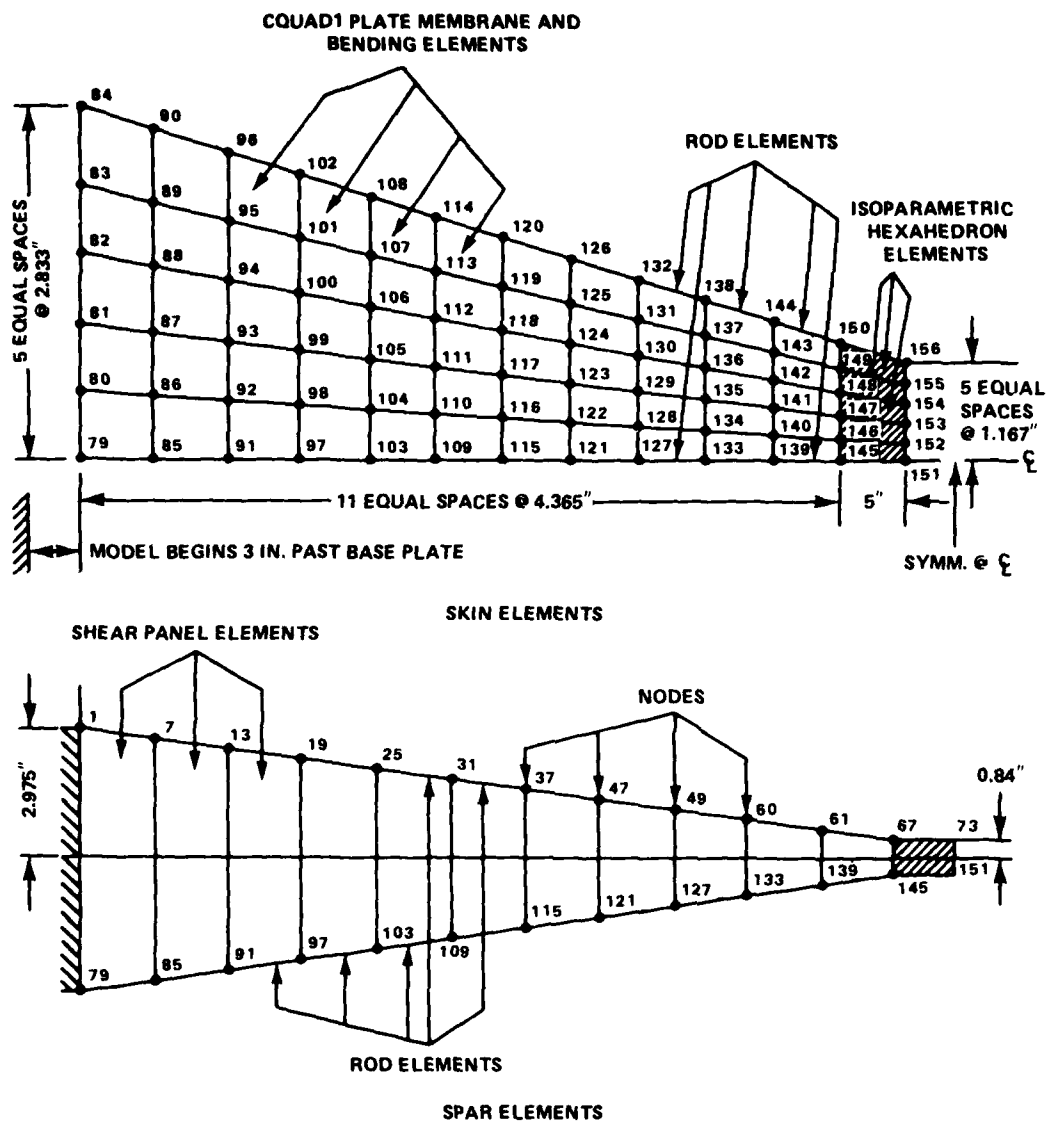Figure 15 - NASTRAN Finite-Element Model for Composite Box Beam

analysis that the CQUAD1 element could be used to model the laminated skin as an equivalent (nonlaminated) skin having the same thickness and same anisotropic elastic properties under membrane and bending action. (Transverse shear stiffness was assumed to be infinite.) This approach was therefore followed in the box beam analysis.

40

From a structural point of view, the NASTRAN membrane plate element CQDMEM could have been used for modeling the box beam skin since the local bending of the skin is minimal due to the configuration and loading. Instead, the CQUAD1 element with both bending and membrane capacity was chosen because it provided a little additional accuracy, as well as reduced the number of unrestrained degrees of freedom which had to be constrained to avoid singularities. This minimized errors caused by manual restraint of these degrees of freedom. In some applications, such as laminated plates under lateral loads where only bending occurs, the use of CQUAD1 or CQDPLT (with bending capacity only) elements are mandatory.

The NASTRAN element connection card CQUAD1 references a property card PQUAD1 which, in turn, references a material property card MAT2. The MAT2 cards define the material properties for linear, temperature-independent, anisotropic materials. This card requires that the program user specify the elements $G_{ij}$ of the two-dimensional anisotropic stress-strain relations below (see Reference 11, pp. 2.4-143):

$$\begin{Bmatrix} \sigma_1 \\ \sigma_2 \\ \sigma_3 \end{Bmatrix} = \begin{bmatrix} G_{11} & G_{12} & G_{13} \\ G_{12} & G_{22} & G_{23} \\ G_{13} & G_{23} & G_{33} \end{bmatrix} \begin{Bmatrix} \varepsilon_1 \\ \varepsilon_2 \\ \gamma_{12} \end{Bmatrix}$$

The elements $G_{ij}$ of the stress-strain relations are synonymous with the variable $\overline{Q}_{ij}^{*}$ which is used in this report and which is also common terminology in laminated plate theory.[5] It is important to distinguish the reduced stiffnesses $G_{ij}$ above, as used in NASTRAN, from shear moduli. The only exception is that the reduced stiffness $G_{33}$ (as defined in NASTRAN, but not in this report) turns out to be the shear modulus $G_{12}$ for a unidirectional lamina (see Appendix A). The procedure for determining the $G_{ij}$ or $Q_{ij}^{*}$ consists of the following steps:

1. The elements $\overline{Q}_{ij}$ of the two-dimensional stress-strain relations (Equations (4) given earlier)

$$\begin{Bmatrix} \sigma_x \\ \sigma_y \\ \tau_{xy} \end{Bmatrix} = \begin{bmatrix} \overline{Q}_{11} & \overline{Q}_{12} & \overline{Q}_{16} \\ \overline{Q}_{12} & \overline{Q}_{22} & \overline{Q}_{26} \\ \overline{Q}_{16} & \overline{Q}_{26} & \overline{Q}_{66} \end{bmatrix} \begin{Bmatrix} \varepsilon_x \\ \varepsilon_y \\ \gamma_{xy} \end{Bmatrix}$$

are first determined for the individual layers of the laminate using the procedure in Appendix A.

2. The $\overline{Q}_{ij}$ from step (1) are next used in Equations (3) to calculate the extensional and bending stiffnesses $A_{ij}$ and $D_{ij}$ for the full laminate, as described in Appendix B.

3. Lastly, reduced stiffnesses $Q^*_{ij(m)}$ and $Q^*_{ij(b)}$ for the full laminate are found from the $A_{ij}$ and $D_{ij}$ using the two equations (see Appendix E)

$$Q^*_{ij(m)} = A_{ij}/h$$

and

$$Q^*_{ij(b)} = D_{ij}/(h^3/12) \tag{30}$$

where h is the thickness of the laminate.

Following the procedure outlined above, the $Q^*_{ij(m)}$ and $Q^*_{ij(b)}$ for the laminated graphite epoxy skin of the box beam were found to be

$$Q^*_{ij(m)} = \begin{bmatrix} 0.17002\times10^8 & 0.44043\times10^7 & 0.18775\times10^6 \\ 0.44043\times10^7 & 0.55951\times10^7 & 0.18776\times10^6 \\ 0.18775\times10^6 & 0.18776\times10^6 & 0.47976\times10^7 \end{bmatrix}$$

and

$$Q^*_{ij(b)} = \begin{bmatrix} 0.16597\times10^8 & 0.48865\times10^7 & -0.61273\times10^1 \\ 0.48865\times10^7 & 0.60800\times10^7 & 0.61273\times10^1 \\ -0.61273\times10^1 & 0.61273\times10^1 & 0.52632\times10^7 \end{bmatrix} \tag{31}$$

In many laminate applications the $Q^*_{ij(m)}$ and $Q^*_{ij(b)}$ will turn out to be similar in value, as was the case for the box beam laminate. Greater differences in magnitude for these reduced laminate stiffnesses may be expected when the individual layers of a laminate have more widely varying stiffness properties. For example, if a laminate is fabricated of rubber and steel layers, with the steel placed in the outer layers

42

of the laminate, the $Q^*_{ij(m)}$ and $Q^*_{ij(b)}$ will exhibit greater differences. Another way of looking at it is that the $D_{ij}$ (and therefore $Q^*_{ij(b)}$) are sensitive to the stacking sequence of the laminas while the $A_{ij}$ (and therefore $Q^*_{ij(m)}$) are not.

Other Modeling Considerations. The box beam skin in the vicinity of its fixed end presents special modeling considerations because of a scarf joint (see detail A of Figure 1) at that location, which involves a hybrid cross section made up of both composite and steel materials. This was solved by use of a "weighting" formula that combines proportionate effects from both steel and composite for a cross section to arrive at the membrane and bending stress-strain relationships. At the opposite free end of the beam, referred to as the load block end, the entire load block region (steel and composite) is considered equivalent to an all steel block, for simplification of the analysis, since the major part is steel. This load block was modeled with isoparametric hexahedron elements, as indicated in Figure 15.

Finally, some comments are made with respect to boundary conditions. When the box beam is viewed from the side (see Figure 1), it is noticed that a massive metal cross section extends a few inches from the base plate. To simplify the model, fixed end conditions are imposed at the cross section where this steel sleeve section ends and the spars and skin continue. This eliminates complexity of the model by excluding a section that would experience relatively little deformation under the applied load. Symmetry of the beam suggests a further reduction of the model by eliminating half of the beam split lengthwise along its longitudinal axis. This artificial boundary is fixed against transverse displacement and rotation about the longitudinal axis so that behavior is consistent in the absence of the other half. All nodes of the structure are fixed against rotations about axes normal to the plate elements because these elements do not offer resistance to this type of displacement and singularities would result if these were not constrained. The isoparametric hexahedron elements pose a similar problem to the plate elements, except no rotational degrees of freedom are allowed. Therefore the nodes bordering these elements are fixed for rotation about all of the space axes.

Technique Effectiveness. Using the NASTRAN model just described, a finite-element analysis was performed on the composite box beam for a 56-kip end load. The analysis

43

results were useful in that they (a) provided a check on the strength-of-material calculation, (b) provided detailed results on the structural behavior of the composite box beam, and (c) demonstrated the utility of the NASTRAN and other similar finite-element computer programs for the analysis of hybrid structures involving composite laminates.

A detailed discussion of the analysis results is provided elsewhere.*,** The aim of this report is to present the finite-element technique for laminated composites and to provide a demonstration of the effectiveness of this technique for hybrid structure such as the composite box beam.

The longitudinal bending stresses in the composite skin and steel spar of the box beam are presented in Figure 16 as obtained from the NASTRAN analysis, strength-of-materials calculations, and static tests. Comparing these results for the laminated skin, it is seen that the NASTRAN curve is in very good agreement with the test data. Similar, and possibly a little closer, agreement was found for the flange of the steel spar. The strength-of-materials curve in Figure 16 is seen to underpredict the test data by approximately 5.5 percent at about 35.0 in. from the fixed end where the governing stresses were obtained. These comparisons demonstrate the effectiveness of the finite-element approach described earlier for composite laminates and also show that conventional strength-of-materials calculations are effective tools for stress prediction in laminates.

Since the laminate stresses in Figure 16 represent, in a sense, averaged values or equivalent material values for a box beam skin having equivalent anisotropic properties, the stresses are not necessarily the maximum values which might occur in any of the layers. For example, the stresses in the first or outer layer of the skin laminate may exceed the equivalent material or averaged stresses for the entire laminate. The procedure for computing the stresses in any layer of the laminate is given in Appendix F.

While the stresses resulting from the finite-element analyses were only averaged values for the laminate skin and required further processing to get individual layer stresses, the nodal point deflections resulting from the analysis (see Figure 17) represent the actual deflections and need no further processing.

---

*Stein, M.C., "A Nastran Analysis of a Composite Laminate Box Beam for Application to Navy Hydrofoils," reported informally as enclosure (1) to DTNSRDC ltr 77-173-186 of 9 Dec 1977.

**Barry, M. and W. Couch. "Advanced Composite Box Beam: Static and NDE Test and Evaluation" (in preparation).

44
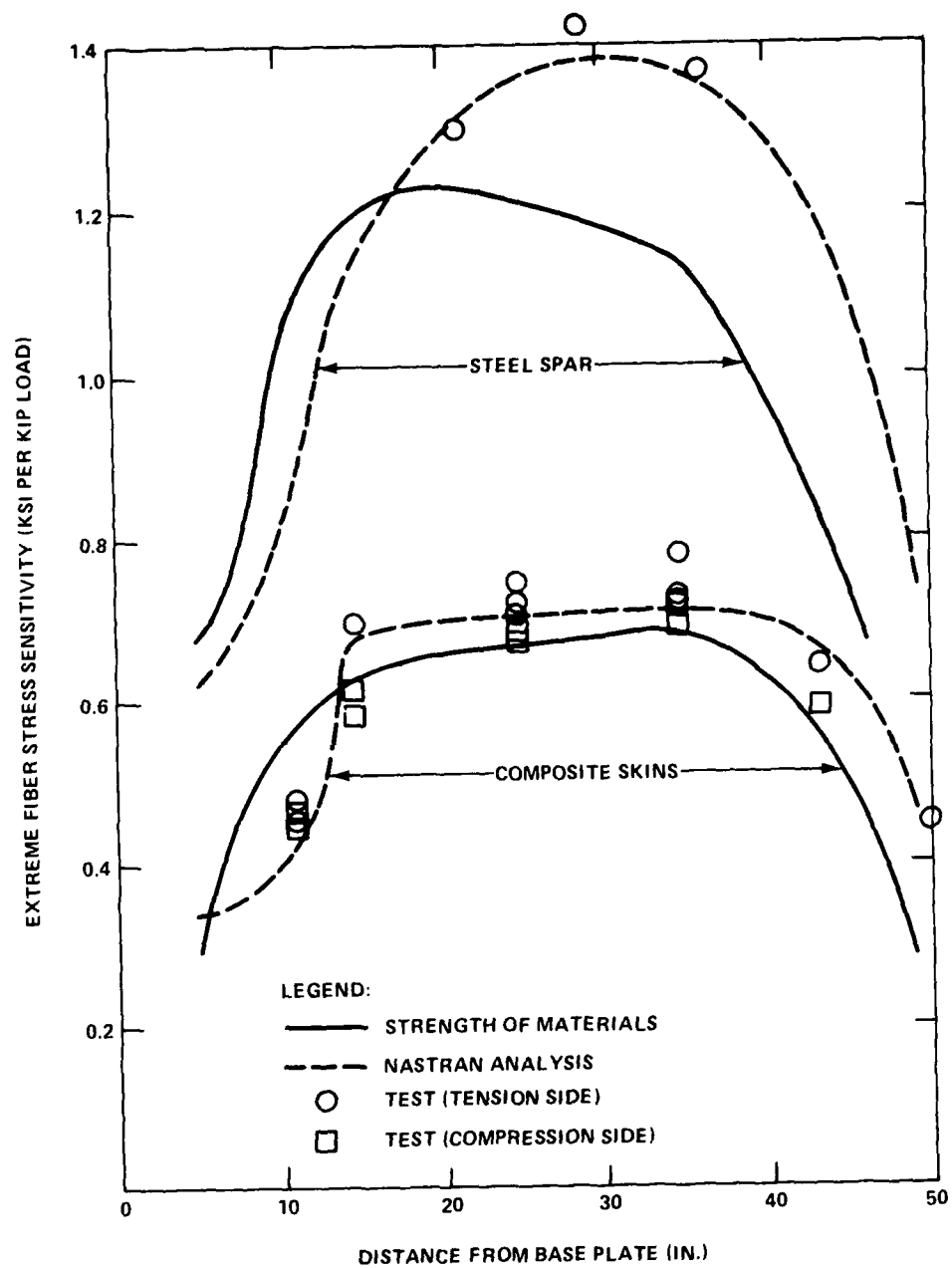
Figure 16 – Comparison of Longitudinal Bending Stresses in
Composite Box Beam Based on Analyses and Tests

45
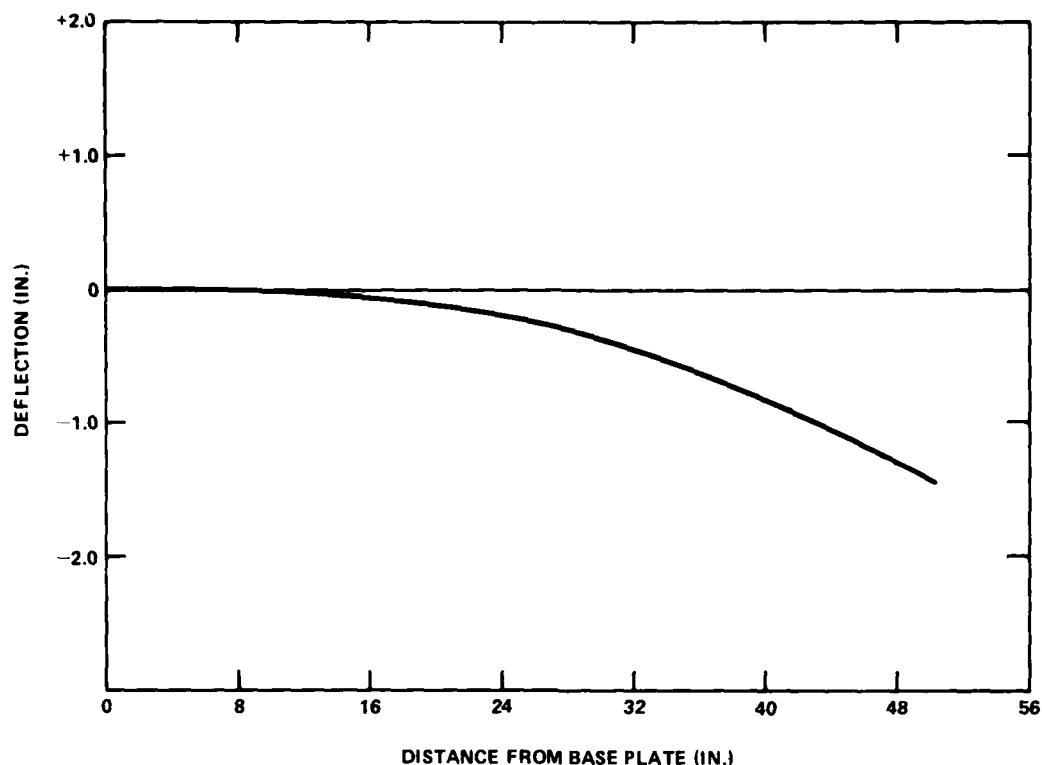
Figure 17 - Deflection Curve for Composite Box Beam with a 56-Kip Load

Foil Flap Analysis

The finite-element procedure applied to the composite box beam and discussed in the previous section was also used to analyze the composite flap for the aft foil of the hydrofoil PCH-1. The composite flap, illustrated in Figure 2, consists of a laminated skin with a titanium crank spar substructure assembly. The composite skin is 1/2 in. thick and is made up of 36 plies of a graphite epoxy fabric (T300) oriented at ±45 deg and clad by 10 mils of titanium.

This report does not discuss results of the foil flap analyses since they are given in Reference 2. Instead, some of the significant differences in structural loading, modeling, and response of the laminated skin in the foil flap and the box beam are pointed out here. Some comments are first made with respect to the box beam. Because of the end loading on the box beam, the laminates in the upper and lower skins or flanges are subjected to longitudinal strains which vary only slightly

46

through the thickness of the skin. Since the in-plane longitudinal strains, as well as the transverse and shear strains, are essentially uniform through the skin thickness, a membrane-type plate element CQDMEM could probably have been used in the NASTRAN analyses. Instead, the CQUAD1 element was employed, with both membrane and bending capacity, to improve the accuracy slightly, but mainly to reduce the number of degrees of freedom which had to be otherwise constrained, as mentioned earlier.

Although the CQUAD1 element may have been somewhat optional in modeling the box beam skin, this element was necessary for representing the foil flap skin in order to accommodate the mostly local bending response associated with the distributed pressure loading on the foil flap.

Another difference between the models for the laminated skin of the foil flap and the box beam has to do with the comparative magnitudes of the reduced stiffnesses $Q^*_{ij(m)}$ and $Q^*_{ij(b)}$. The greatest difference in these reduced stiffnesses for the box beam was only 2.4 percent ($Q^*_{11(b)} = 17.002 \times 10^6$ and $Q^*_{11(m)} = 16.597 \times 10^6$). With so little difference, the membrane reduced stiffness could have been input for both the membrane and bending components of the CQUAD2 element without much loss in accuracy. However, in the case of the laminated foil flap skin, the greatest difference in magnitude between $Q^*_{ij(b)}$ and $Q^*_{ij(m)}$ was found to be 13.5 percent ($Q^*_{11(b)} = 7.506 \times 10^6$ and $Q^*_{11(m)} = 6.616 \times 10^6$). Therefore, it is more important for the foil flap analysis than it was for the box beam that the distinct values for $Q^*_{ij(b)}$ and $Q^*_{ij(m)}$ be used.

## SUMMARY AND CONCLUSIONS

Since the liklihood exists that laminated composites will be increasingly used in the fabrication of ship and marine structures in general, it is important that appropriate design and analytical methods be available for supporting their application.

Relatively recent applications of laminated composites in the U.S. Navy have included the forward foil test component and the control flap on the foil of the hydrofoil PCH-1. It is possible that future applications could eventually include some of the other basic components of ship structure, such as stiffeners, girders, stanchions, shell, and bulkhead plating. All of these past and future applications may be modeled and analyzed as one of the laminated structural components (i.e., laminated beam, column, plate, panels, or grillage. . . see Figure 4).

Three types of analytical methods which are commonly applied to metallic structures have been extended to laminated composite applications. These include (Table 1): strength-of-materials techniques; classical methods for the bending, buckling, and vibration of laminated plates; and finite-element and finite-difference methods. In order to apply these methods to laminated composites, it is necessary to represent the laminated member by an equivalent nonlaminated member having equivalent elastic properties.

Corresponding to each of the three types of analytical methods there are three kinds of elastic properties which must be evaluated in advance by the structural analyst. The required stiffness properties are: engineering constants $E_x$, $E_y$, $\nu_{xy}$, $\nu_{yx}$, and $G_{xy}$ for strength-of-materials analyses; extensional and bending stiffnesses $A_{ij}$ and $D_{ij}$ for classical plate analyses; and reduced stiffnesses $Q_{ij}^*$ for finite-element analyses. These three sets of stiffness parameters are not independent but are analytically related and derived from each other. Extensional and bending stiffnesses are normally calculated first and then used to compute the engineering constants and the reduced stiffnesses as needed. Since the computation of these equivalent stiffnesses is a tedious procedure, if performed manually for a laminate of many layers, computer programs have been written to automate the procedure. One nonproprietary program which is readily available to the public is SQ5 (see Appendix D). If one chooses to perform these calculations manually for a laminate of only a few layers, or if one wants to better understand the theory behind the stiffness calculations, then refer to Appendices A, B, C, and E. As an illustration of the manual process for computing engineering constants, calculations are given in Appendix C for the laminated skin of a composite box beam (for application to the forward foil of the PCH-1 hydrofoil) consisting of 53 plies of T300 graphite fibers and 32 plies of GY70 fibers. These constants were found to be in close agreement with experimentally measured engineering constants, as indicated in Table 2. This result demonstrates that the equivalent engineering constants for multilayered laminates may be adequately determined analytically without resorting to more costly experimental means. It should be noted, however, that it is common practice to use experimental measurements to determine the unidirectional elastic moduli for the constituent layers within the laminate since existing analytical procedures such as the "law of mixtures" are not always of sufficient accuracy. The law of mixtures[5] simply computes the unidirectional elastic modulus of a fiber-imbedded layer from

48

the elastic moduli of the fiber and matrix materials and the percentage composition of each. It is important to note that in determining the equivalent stiffnesses for a laminate, a distinction is made between equivalent stiffness properties under extensional and bending responses. For example, the engineering constants shown in Table 2, and referred to above, are based on a purely extensional response of the box beam laminate.

As mentioned above, three types of analytical methods are discussed in this report for analyzing the structural response of hybrid structures involving composite laminates. Solution methods are discussed for analyzing laminated beams, columns, and rectangular plates. In the case of plates, engineering formulas are readily available for evaluating the deflection, buckling, and vibration behavior of simply supported rectangular plates where the laminate construction consists of a cross-ply arrangement (Figure 7). For plates having angle-ply layups, the analyst must develop desired solutions by using the governing differential equations and boundary conditions.

The finite-element method is the most general tool for analyzing the structural response of laminates. At least four finite-element approaches are available, as illustrated in Figure 14, for investigating laminates depending on the type of stress results desired. The first approach involves the modeling of laminates using 2D plate elements where different equivalent stiffness properties are allowed for membrane and bending. This approach, which was successfully employed and validated on the composite box beam, results in determination of in-plane normal end shear stresses within the laminate. These stress results correlated well with test results and strength-of-materials calculations. The finite-element analysis itself produces equivalent stresses for the full laminate, but these may be further processed to give stresses within the individual layers of the laminate. If a knowledge of the interlaminar shear and through-the-thickness normal stresses is required, as is frequently the case for many applications, one of the other three approaches in Figure 14 must be implemented.

## ACKNOWLEDGMENTS

# APPENDIX A

## REDUCED STIFFNESSES FOR INDIVIDUAL LAMINAS

### A.1. REDUCED STIFFNESSES FROM UNIDIRECTIONAL MODULI

The theory below applies for a single lamina or layer of a composite laminate having fibers imbedded in one direction only (see sketch).

Once the unidirectional elastic constants $E_1$, $E_2$, $\nu_{12}$, $\nu_{21}$, and $G_{12}$ are available from coupon tests for a given individual lamina, the two-dimensional (2D) stress-strain relations may be obtained in terms of these constants from

$$\left\{ \begin{array}{c} \sigma_1 \\ \sigma_2 \\ \tau_{12} \end{array} \right\} = \begin{bmatrix} Q_{11} & Q_{12} & 0 \\ Q_{12} & Q_{22} & 0 \\ 0 & 0 & Q_{66} \end{bmatrix} \left\{ \begin{array}{c} \varepsilon_1 \\ \varepsilon_2 \\ \gamma_{12} \end{array} \right\} \tag{A.1}$$

where the $Q_{ij}$, the reduced stiffnesses, are given by

$$Q_{11} = \frac{E_1}{1 - \nu_{12}\,\nu_{21}}$$

$$Q_{12} = \frac{\nu_{12}\,E_2}{1 - \nu_{12}\,\nu_{21}} = \frac{\nu_{21}\,E_1}{1 - \nu_{12}\,\nu_{21}}$$

$$Q_{22} = \frac{E_2}{1 - \nu_{12}\,\nu_{21}}$$
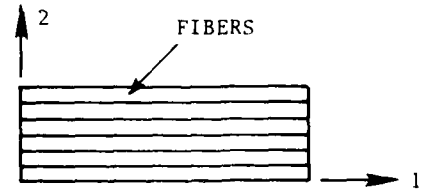
and

$$Q_{66} = G_{12}$$

### A.2. TRANSFORMATION OF REDUCED STIFFNESSES TO DIRECTION OF LOADING

Since the individual laminas may be stacked up at nonzero (45 deg, as an example) angles to the direction of loading to achieve desired strength and stiffness

for the overall laminate, it is necessary that the 2D stress-relations Equation (A.1) for the laminas having fibers oriented at some angle to the direction of loading be transformed to the direction of loading on the laminate. The transformed stress-strain relations have the form

$$
\begin{Bmatrix} \sigma_x \\ \sigma_y \\ \tau_{xy} \end{Bmatrix} = \begin{bmatrix} \overline{Q}_{11} & \overline{Q}_{12} & \overline{Q}_{16} \\ \overline{Q}_{12} & \overline{Q}_{22} & \overline{Q}_{26} \\ \overline{Q}_{16} & \overline{Q}_{26} & \overline{Q}_{66} \end{bmatrix} \begin{Bmatrix} \varepsilon_x \\ \varepsilon_y \\ \gamma_{xy} \end{Bmatrix}
$$

where the transformed reduced stiffnesses $\overline{Q}_{ij}$ are computed from

$$\overline{Q}_{11} = U_1 + U_2 \cos 2\theta + U_3 \cos 4\theta$$

$$\overline{Q}_{12} = U_4 - U_3 \cos 4\theta$$

$$\overline{Q}_{22} = U_1 - U_2 \cos 2\theta + U_3 \cos 4\theta$$

$$\overline{Q}_{16} = -\frac{1}{2} U_2 \sin 2\theta - U_3 \sin 4\theta$$

$$\overline{Q}_{26} = -\frac{1}{2} U_2 \sin 2\theta + U_3 \sin 4\theta$$
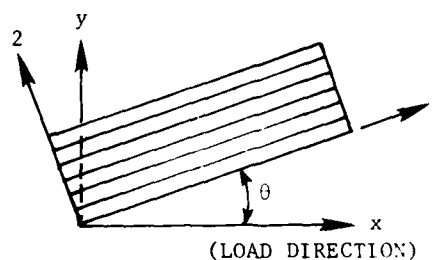
and

$$\overline{Q}_{66} = U_5 - U_3 \cos 4\theta$$

in which

$$U_1 = \frac{3Q_{11} + 3Q_{22} + 2Q_{12} + 4Q_{66}}{8}$$

$$U_2 = \frac{Q_{11} - Q_{22}}{2}$$

$$U_3 = \frac{Q_{11} + Q_{22} - 2Q_{12} - 4Q_{66}}{8}$$

$$U_4 = \frac{Q_{11} + Q_{22} + 6Q_{12} - 4Q_{66}}{8}$$

and

$$U_5 = \frac{Q_{11} + Q_{22} - 2Q_{12} + 4Q_{66}}{8}$$

BLANK PAGE

# APPENDIX B

## LAMINATE EXTENSIONAL AND BENDING STIFFNESSES

As was discussed earlier in the main text, the extensional and bending stiffnesses $A_{ij}$ and $D_{ij}$, respectively, for a laminate are expressed by (assuming a symmetric layup about the midplane so that $B_{ij} = 0$)

$$A_{ij} = \int_{-h/2}^{h/2} \overline{Q}_{ij}\, dz = \sum_{k=1}^{N} (\overline{Q}_{ij})_k\, (z_k - z_{k-1})$$

and (B.1)

$$D_{ij} = \int_{-h/2}^{h/2} \overline{Q}_{ij}\, z^2 dz = \frac{1}{3}\sum_{k=1}^{N} (\overline{Q}_{ij})_k\, (z_k^3 - z_{k-1}^3)$$

Once the transformed reduced stiffnesses $\overline{Q}_{ij}$ have been found using the procedure of Appendix A, the task of finding $A_{ij}$ and $D_{ij}$ above entails carrying out the indicated summations involving the $\overline{Q}_{ij}$ for each lamina and the distances to the upper and lower surfaces of the laminas, $z_{k-1}$ and $z_k$, respectively (see sketch below).

The task of computing the $A_{ij}$ and $D_{ij}$ using Equations (B.1) for a laminate with many layers is a tedious one and well suited for the computer, especially the $D_{ij}$.

DETERMINING $A_{ij}$

The summation process in Equation (B.1) for determining $A_{ij}$ is illustrated below for a laminate with four layers having symmetry about the midplane.

$$
\begin{aligned}
A_{ij} = \quad & (\overline{Q}_{ij})_1\, (z_1 - z_0) \\
+ & (\overline{Q}_{ij})_2\, (z_2 - z_1) \\
+ & (\overline{Q}_{ij})_3\, (z_3 - z_2) \\
+ & (\overline{Q}_{ij})_4\, (z_4 - z_3)
\end{aligned}
$$

(B.2)



55
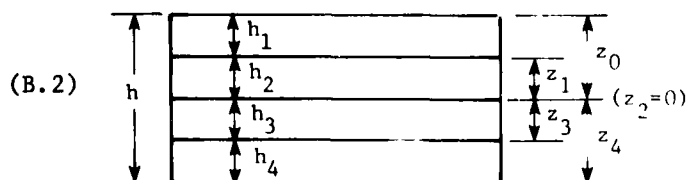
For the case where the four layers are of equal thickness (h/4),

$$z_0 = -h/2$$
$$z_1 = -h/4$$
$$z_2 = 0 \qquad\qquad (B.3)$$
$$z_3 = +h/4$$
$$z_4 = +h/2$$

Therefore,

$$A_{ij} = (\overline{Q}_{ij})_1 h/4 + (\overline{Q}_{ij})_2 h/4 + (\overline{Q}_{ij})_3 h/4 + (\overline{Q}_{ij})_4 h/4$$

$$= [(\overline{Q}_{ij})_1 + (\overline{Q}_{ij})_2 + (\overline{Q}_{ij})_3 + (\overline{Q}_{ij})_4] \, h/4 \qquad (B.4)$$

For the case when the laminate thicknesses $h_1$ through $h_4$ are all different,

$$A_{ij} = (\overline{Q}_{ij})_1 \, h_1 + (\overline{Q}_{ij})_2 \, h_2 + (\overline{Q}_{ij})_3 \, h_3 + (\overline{Q}_{ij})_4 \, h_4 \qquad (B.5)$$

However, for laminates having a symmetric layup (such that the coupling stiffnesses $B_{ij} = 0$, as assumed earlier),

$$h_1 = h_4 = h_a \qquad (\overline{Q}_{ij})_1 = (\overline{Q}_{ij})_4 = (\overline{Q}_{ij})_a$$
$$\qquad\qquad (B.6)$$
$$h_2 = h_3 = h_b \qquad (\overline{Q}_{ij})_2 = (\overline{Q}_{ij})_3 = (\overline{Q}_{ij})_b$$

In this case,

$$A_{ij} = 2(\overline{Q}_{ij})_a \, h_a + 2(\overline{Q}_{ij})_b \, h_b \qquad (B.7)$$

56

## DETERMINING $D_{ij}$

The bending stiffness $D_{ij}$ is given by the following summation for the four-layer laminate previously considered where the four layers are of equal thickness $h/4$:

$$D_{ij} = \frac{1}{3}(\overline{Q}_{ij})_1 (z_1^3 - z_0^3) + \frac{1}{3}(\overline{Q}_{ij})_2 (z_2^3 - z_1^3)$$

$$\text{(B.8)}$$

$$+ \frac{1}{3}(\overline{Q}_{ij})_3 (z_3^3 - z_2^3) + \frac{1}{3}(\overline{Q}_{ij})_4 (z_4^3 - z_3^3)$$

Substituting $z_1$ through $z_4$ in terms of $h$ from Equations (B.3), there results

$$D_{ij} = [7(\overline{Q}_{ij})_1 + (\overline{Q}_{ij})_2 + (\overline{Q}_{ij})_3 + 7(\overline{Q}_{ij})_4] \frac{h^3}{192}$$

For the case where all four layers are of unequal thickness, the $D_{ij}$ counterpart of Equation (B.5) for $A_{ij}$ may be written down, but not as concisely as Equation (B.5). Recall from before that the absence of symmetry in the layer thicknesses or the $\overline{Q}_{ij}$ about the midsurface of the laminate will necessitate the computation of the $B_{ij}$ from Equation (3) since they are no longer zero. However, in most structural designs, the laminates are designed with built-in symmetry to reduce the complexity of the structural analyses needed to assess structural performance and integrity.

BLANK PAGE

# APPENDIX C

## NUMERICAL EXAMPLE: COMPUTATIONS FOR HYBRID BOX BEAM LAMINATE

### DESCRIPTION OF HYBRID LAMINATE

- Composition

    53 plies of T300 graphite fibers at 0° to loading
        direction (ply thickness = 0.00516 in.)

    32 plies of GY70 graphite fibers at ±45° to loading
        direction (ply thickness = 0.00692 in.)

" Stacking Sequence

    $0°$, $(0_3°, \pm45°)_8$, $0_3°$, $(\overline{+45}°, 0_3°)_8$, $0°$

### C.1. EXTENSIONAL STIFFNESSES

Engineering Constants for Unidirectionally Reinforced Lamina (from Reference 1):

| Constant | T300 Ply | GY70 Ply |
|----------|----------|----------|
| $E_1$ | $20.41\times10^6$ psi | $42.9\times10^6$ psi |
| $E_2$ | $1.42\times10^6$ psi | $0.89\times10^6$ psi |
| $\nu_{12}$ | $0.181^*$ | $0.482^*$ |
| $\nu_{21}$ | $0.0126$ | $0.010$ |
| $G_{12}$ | $0.792\times10^6$ psi | $0.614\times10^6$ psi |

*Computed from $\nu_{12} = \nu_{21} E_1/E_2$.

<u>Reduced Stiffnesses for Unidirectionally Reinforced Lamina (see procedure in Appendix A, Section A.1):</u>

| Stiffness | T300 Ply | GY70 Ply |
|---|---|---|
| $Q_{11} = \dfrac{E_1}{(1-\nu_{12}\,\nu_{21})}$ | $20.457 \times 10^6$ | $43.108 \times 10^6$ |
| $Q_{12} = \dfrac{\nu_{12}\,E_2}{(1-\nu_{12}\,\nu_{21})}$ | $0.258 \times 10^6$ | $0.431 \times 10^6$ |
| $Q_{22} = \dfrac{E_2}{(1-\nu_{12}\,\nu_{21})}$ | $1.423 \times 10^6$ | $0.894 \times 10^6$ |
| $Q_{66} = G_{12}$ | $0.792 \times 10^6$ | $0.614 \times 10^6$ |

<u>Transformation of Reduced Stiffnesses to Direction of Loading (see procedure in Appendix A, Section A.2):</u>

<u>T300 Plies</u>: Since T300 plies are already oriented in the direction of loading, no transformation of the $Q_{ij}$ for T300 is necessary. Therefore, $\overline{Q}_{ij} = Q_{ij}$.

<u>GY70 Plies</u>: Substituting the $Q_{ij}$ values from above,

$$U_1 = (3Q_{11} + 3Q_{22} + 2Q_{12} + 4Q_{66})/8 = 16.91555 \times 10^6$$

$$U_2 = (Q_{11} - Q_{22})/2 = 21.10674 \times 10^6$$

$$U_3 = (Q_{11} + Q_{22} - 2Q_{12} - 4Q_{66})/8 = 5.08550 \times 10^6$$

$$U_4 = (Q_{11} + Q_{22} + 6Q_{12} - 4Q_{66})/8 = 5.51656 \times 10^6$$

and

$$U_5 = (Q_{11} + Q_{22} - 2Q_{12} + 4Q_{66})/8 = 5.69950 \times 10^6$$

60

Then, for plies with fibers at $\theta = +45$ deg,

$$\overline{Q}_{11} = U_1 + U_2 \cos2\theta + U_3 \cos4\theta = 11.83005 \times 10^6$$

$$\overline{Q}_{12} = U_4 - U_3 \cos4\theta = 10.60206 \times 10^6$$

$$\overline{Q}_{22} = U_1 - U_2 \cos2\theta + U_3 \cos4\theta = 11.83005 \times 10^6$$

$$\overline{Q}_{16} = -\frac{1}{2} U_2 \sin2\theta - U_3 \sin4\theta = -10.55337 \times 10^6$$

$$\overline{Q}_{26} = -\frac{1}{2} U_2 \sin2\theta + U_3 \sin4\theta = -10.55337 \times 10^6$$

and

$$\overline{Q}_{66} = U_5 - U_3 \cos4\theta = 10.78500 \times 10^6$$

For the plies having fibers at $\theta = -45$ deg,

$$\overline{Q}_{11} = 11.83005 \times 10^6$$

$$\overline{Q}_{12} = 10.60206 \times 10^6$$

$$\overline{Q}_{22} = 11.83005 \times 10^6$$

$$\overline{Q}_{16} = 10.55337 \times 10^6$$

$$\overline{Q}_{26} = 10.55337 \times 10^6$$

and

$$\overline{Q}_{66} = 10.78500 \times 10^6$$

Determination of Extensional Stiffnesses $A_{ij}$: Extensional stiffnesses $A_{ij}$ are determined using Equation (B.1) (also see Equations (B.2) and (B.3) for examples illustrating the use of Equation (B.1)) as follows:

$$A_{ij} = \overline{Q}_{ij_{T300(0°)}} h_{(T300)} + \overline{Q}_{ij_{GY70(+45°)}} h_{(+45°)} + \overline{Q}_{ij_{GY70(-45°)}} h_{(-45°)}$$

61

Now,

$$h_{(T300)} = 53 \text{ plies} \times 0.00516 \text{ in./ply} = 0.27348 \text{ in.}$$

and

$$h_{(+45°)} = h_{(-45°)} = 16 \text{ plies} \times 0.00692 \text{ in./ply} = 0.11072 \text{ in.}$$

Therefore,

$$A_{ij} = \overline{Q}_{ij_{T300(0°)}} (0.27348) + \overline{Q}_{ij_{GY70(+45°)}} (0.11072) + \overline{Q}_{ij_{GY70(-45°)}} (0.11072)$$

and

$$A_{11} = [(20.457)(0.27348) + (11.83005)(0.11072) + (11.83005)(0.11072)] \times 10^6$$

$$= 8.21423 \times 10^6$$

Similarly,

$$A_{12} = 2.41828 \times 10^6$$

$$A_{22} = 3.00881 \times 10^6$$

$$A_{16} = 0.0$$

$$A_{26} = 0.0$$

and

$$A_{66} = 2.60483 \times 10^6$$

C.2. ENGINEERING CONSTANTS FOR TOTAL LAMINATE

Inverse of Extensional Stiffness Matrix $\overline{A}_{ij}$:  Substituting values for $A_{ij}$ into Equation (7) gives

$$\Delta = A_{11}(A_{22} A_{66} - A_{26}^2) - A_{12}(A_{12} A_{66} - A_{16} A_{26}) + A_{16}(A_{12} A_{26} - A_{16} A_{22})$$

$$= 49.1453 \times 10^{18}$$

Then,

$$\bar{A}_{11} = (A_{22} A_{66} - A_{26}^2)/\Delta = 1.59475 \times 10^{-7}$$

$$\bar{A}_{12} = - (A_{12} A_{66} - A_{16} A_{26})/\Delta = -1.28175 \times 10^{-7}$$

$$\bar{A}_{22} = (A_{11} A_{66} - A_{16}^2)/\Delta = 4.35376 \times 10^{-7}$$

$$\bar{A}_{16} = (A_{12} A_{26} - A_{16} A_{22})/\Delta = 0$$

$$\bar{A}_{26} = - (A_{11} A_{26} - A_{16} A_{12})/\Delta = 0$$

and

$$\bar{A}_{66} = (A_{11} A_{22} - A_{12}^2)/\Delta = 3.83902 \times 10^{-7}$$

Determination of Engineering Constants: Inserting the values of $\bar{A}_{ij}$ above into Equations (9) and rounding off the numerical results gives

$$E_x = 1/(\bar{A}_{11} h) = 12.67 \times 10^6 \text{ psi}$$

$$E_y = 1/(\bar{A}_{22} h) = 4.64 \times 10^6 \text{ psi}$$

$$G_{xy} = 1/(\bar{A}_{66} h) = 5.26 \times 10^6 \text{ psi}$$

$$\nu_{xy} = -\bar{A}_{12}/\bar{A}_{11} = 0.804$$

$$\nu_{yx} = -\bar{A}_{12}/\bar{A}_{22} = 0.294$$

$$\eta_{xy,x} = \bar{A}_{16}/\bar{A}_{11} = 0$$

$$\eta_{xy,y} = \bar{A}_{26}/\bar{A}_{22} = 0$$

$$\eta_{x,xy} = \bar{A}_{16}/\bar{A}_{66} = 0$$

and

$$\eta_{y,xy} = \bar{A}_{26}/\bar{A}_{66} = 0$$

BLANK PAGE

## APPENDIX D

### INPUT DATA FOR COMPUTER PROGRAM SQ5

The general content of each card (from Reference 7) in the SQ5 problem deck is as follows:

| CARD | COLUMNS | FORMAT | VARIABLE | REMARKS |
|---|---|---|---|---|
| 1 | 1 | Blank | -- | -- |
|  | 2-66 | A65 | Title | Any alphanumeric information describing the problem which will be printed at the top of the first page of the problem output. |
| 2 | 1-5 |  | Key 1= | 0--Program operation continues after computation of laminate data.<br><br>1--Program terminates after computing and writing out the elements of the constitutive matrices and the average laminate properties. |
|  | 6-10 |  | Key 2= | 0--No point stress or thermal analysis will be done.<br><br>1--A point stress analysis will be made on input sets of $N_x$, $N_y$, and $N_{xy}$. One card per load case must be added to the problem deck (see Card 6). This key must be set to 1 if a thermal analysis is to be performed. |
|  | 11-15 | I5 | Key 3= | 0--No additional analysis to be performed.<br><br>1--A point stress analysis will be made of average stresses $\sigma_\alpha$, $\sigma_\beta$, $\tau_{\alpha\beta}$, and $\theta$. $\theta$ is the angle at which the stresses are applied. This analysis is for in-plane loads only.<br><br>2--An interaction diagram will be computed for the input laminate. |

| CARD | COLUMNS | FORMAT | VARIABLE | REMARKS |
|------|---------|--------|----------|---------|
| | 16-20 | | Key 4= | 0--No thermal analysis will be made. |
| | | | | 1--Thermally induced in-plane stress $N_x^T$, $N_y^T$, $N_{xy}^T$ and moment $M_x^T$, $M_y^T$, $M_{xy}^T$ resultants will be computed for an input temperature change. If Key 4 = 1, Key 2 must be set equal to 1. |
| | 21-25 | | Key 5= | 0--No interlaminar shear stress analysis will be made. |
| | | | | 1--An interlaminar shear stress analysis will be made for input values of $Q_x$ and $Q_y$. |
| | 26-30 | | MA | Number of lamina (100 max.). |
| | 31-35 | I5 | NOMAT | Number of materials (100 max.). |
| | 36-40 | | NCL | Number of loading cases. This applies to sets of $N_x$, $N_y$, $N_{xy}$ and $M_x$, $M_y$, $M_{xy}$, temperature changes, and $Q_x$ and $Q_y$ (10 max.). |
| 3 | 1-5 | I5 | KEYNU= | 0--Minor Poisson's ratio of each material is calculated by the program. |
| | | | | 1--Minor Poisson's ratio of each material is input. |
| | 1-9 | | E1(I) | Modulus of elasticity of the I-th material along the first (or "1") lamina axis. |
| | 10-18 | | E2(I) | Modulus of elasticity of the I-th material along the second (or "2") lamina axis which is orthogonal to the "1" lamina axis. |
| | 19-27 | | U1(I) | First or Major Poisson's ratio of the I-th material. |

| CARD | COLUMNS | FORMAT | VARIABLE | REMARKS |
|------|---------|--------|----------|---------|
|  | 28-36 |  | G(I) | Shear modulus of elasticity of the I-th material. |
|  | 37-45 |  | ALPHA 1(I) | Coefficient of thermal expansion of the I-th material in the "1" lamina direction. |
| 4* | 46-54 | F9.0 | ALPHA 2(I) | Coefficient of thermal expansion of the I-th material in the "2" lamina direction. |
|  | 55-63 |  | ALPHA 6(I) | Shearing coefficient of thermal expansion of the I-th material. |
| 5** | 1-9 | F9.0 | U2(I) | Second or minor Poisson's ratio of the I-th material. |
|  | 1-5 | I5 | LAY | Lamina number. |
|  | 6-10 | I5 | MATYPE(I) | Material of I-th lamina. |
| 6*** | 11-20 | F10.0 | TH(I) | Counterclockwise angle in degrees from the laminate reference axes x, y to the lamina natural axes 1, 2 of the I-th lamina. |
|  | 21-30 | F10.0 | AT(I) | Thickness of the I-th lamina. |
|  | 1-10 |  | CALE1(I) | Compression limit strain allowable for the I-th material in the "1" lamina direction. |
|  | 11-20 |  | CALE2(I) | Compression limit strain allowable for the I-th material in the "2" lamina direction. |
| 7 | 21-30 | F10.0 | CALE3(I) | Negative limit shear strain allowable for the I-th material. |
|  | 31-40 |  | TALE1(I) | Tension limit strain allowable for the I-th material in the "1" lamina direction. |

*There will be a Card 4 for each material.

**There will be a Card 5 for each material only if KEYNU = 1 on Card 3.

***There will be a Card 6 for each lamina.

| CARD | COLUMNS | FORMAT | VARIABLE | REMARKS |
|------|---------|--------|----------|---------|
| 7* | 41-50 | | TALE2(I) | Tension limit strain allowable for the I-th material in the "2" lamina direction. |
| | 51-60 | | TALE3(I) | Positive limit shear strain allowable for the I-th material. |
| 8** | 1-9 | | N(I,1) | In-plane force resultant in the x direction for load case I (lb/in.). |
| | 10-18 | | N(I,2) | In-plane force resultant in the y direction for load case I (lb/in.). |
| | 19-27 | | N(I,3) | In-plane shear force resultant for load case I (lb/in.). |
| | 28-36 | F9.0 | M(I,1) | $M_x$ moment resultant for load case I (in.-lb/in.). |
| | 37-45 | | M(I,2) | $M_y$ moment resultant for load case I (in.-lb/in.). |
| | 46-54 | | M(I,3) | $M_{xy}$ moment resultant for load case I (in.-lb/in.). |
| | 55-63 | | T(I) | Change in temperature for load case I. |
| | 1-10 | | SIG1 | Average laminate stress $\sigma_\alpha$ acting in $\alpha$ direction of an $\alpha$, $\beta$ system at an angle PH1 from the laminate x, y axis system. |
| | 11-20 | | SIG2 | Average laminate stress $\sigma_\beta$ acting in $\beta$ direction. |

*There will be a Card 7 for each material.

**There will be a Card 8 for each load case. Card 8 is omitted if (a) only laminate properties are desired, (b) only an interaction diagram is desired, or (c) only an interlaminar shear analysis is desired.

| CARD | COLUMNS | FORMAT | VARIABLE | REMARKS |
|------|---------|--------|----------|---------|
| 9* | 21–30 | F10.0 | SIG3 | Average laminate shearing stress $\sigma_{\alpha\beta}$. |
| | 31–40 | | PH1 | Angle in degrees from the $\alpha$, $\beta$ system to the x, y system. |
| | 1–10 | | QX(1) | X shear force resultant for load case 1 (lb/in.). |
| | 11–20 | | QY(1) | Y shear force resultant for load case 1 (lb/in.). |
| 10** | 21–30 | F10.0 | QX(2) | X shear force resultant for load case 2 (lb/in.). |
| | 31–40 | | QY(2) | Y shear force resultant for load case 2 (lb/in.). |
| | 41–50 | | QX(3) | X shear force resultant for load case 3 (lb/in.). |
| | 51–60 | | QY(3) | Y shear force resultant for load case 3 (lb/in.). |

---

*Card 9 is input only if Key 3 = 1 and Key 1 = Key 2 = Key 4 = 0.

**Enough Card 10's must be included to cover all load cases if Key 5 = 1.

BLANK PAGE

## APPENDIX E

### REDUCED STIFFNESSES OF LAMINATES FOR FINITE-ELEMENT ANALYSES

It was discussed earlier in this report how the reduced stiffnesses $Q_{ij}^*$ for laminates may be used in finite-element programs (such as NASTRAN) to represent the two-dimensional anisotropic elastic behavior of an equivalent nonlaminated material. This appendix outlines the steps for determining these $Q_{ij}^*$ (referred to as $G_{ij}$ on the MAT2 card of NASTRAN).

Consider the laminated plate element, shown on the left in the sketch below, having unit length and width and thickness h. The laminate may have any number of layers, layer thickness, and fiber orientation just so long as the laminate ends up being symmetric about the midplane (so that coupling stiffnesses $B_{ij}$ between extension and bending are zero—see Table 2 earlier in text). The laminated plate element is to be replaced by an equivalent (in the sense that it has the same extensional and bending stiffnesses) nonlaminated plate.
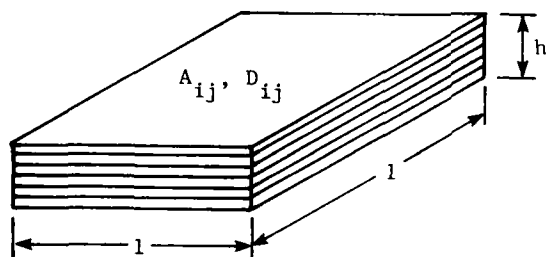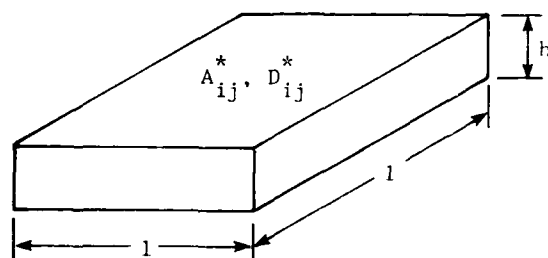


Laminated Plate                    Equivalent Nonlaminated Plate

For the symmetric laminated plate element above, the in-plane forces are related to in-plane strains by

$$\begin{Bmatrix} N_x \\ N_y \\ N_{xy} \end{Bmatrix} = \begin{bmatrix} A_{11} & A_{12} & A_{16} \\ A_{12} & A_{22} & A_{26} \\ A_{16} & A_{26} & A_{66} \end{bmatrix} \begin{Bmatrix} \varepsilon_x \\ \varepsilon_y \\ \gamma_{xy} \end{Bmatrix} \tag{E.1}$$

71

and the moments are related to the out-of-plane curvatures by

$$
\left\{ \begin{matrix} M_x \\ M_y \\ M_{xy} \end{matrix} \right\} = \begin{bmatrix} D_{11} & D_{12} & D_{16} \\ D_{12} & D_{22} & D_{26} \\ D_{16} & D_{26} & D_{66} \end{bmatrix} \left\{ \begin{matrix} k_x \\ k_y \\ k_{xy} \end{matrix} \right\} \tag{E.2}
$$

Or, using condensed matrix notation,

$$
\{N\} = [A]\{\varepsilon\} \quad \text{and} \quad \{M\} = [D]\{k\} \tag{E.3}
$$

Likewise, the force-strain and moment-curvature relations on the laminated plate may be written as

$$
\{N^*\} = [A^*]\{\varepsilon^*\} \quad \text{and} \quad \{M^*\} = [D^*]\{k^*\} \tag{E.4}
$$

where $[A^*]$ and $[D^*]$ are the extensional and bending stiffnesses for the equivalent nonlaminated plate. Now, if for the same applied loads on the laminated and equivalent nonlaminated plate, that is, for

$$
\{N\} = \{N^*\} \quad \text{and} \quad \{M\} = \{M^*\}
$$

the two plates have the same strain and curvature

$$
\{\varepsilon\} = \{\varepsilon^*\} \quad \text{and} \quad \{k\} = \{k^*\}
$$

then it follows that the plates must also have the same extensional and bending stiffnesses

$$
[A] = [A^*] \quad \text{and} \quad [D] = [D^*] \tag{E.5}
$$

Next, using either Equations (3) or (B.1) (both are the same), the stiffnesses $[A^*]$ and $[D^*]$ may be shown to be given by

72

$$[A^*] = [Q_m^*]h$$

and

$$[D^*] = [Q_b^*]h^3/12 \qquad (E.6)$$

Therefore, substituting Equation (E.6) into Equation (E.5), we have

$$[Q_m^*] = [A]\frac{1}{h} \qquad (E.7)$$

and

$$[Q_b^*] = [D]\frac{1}{h^3/12}$$

or

$$Q_{ij}^*{}_{(m)} = A_{ij}/h \qquad (E.8)$$

and

$$Q_{ij}^*{}_{(b)} = 12\ D_{ij}/h^3$$

Using Equation (E.8), the reduced stiffnesses $Q_{ij}^*{}_{(m)}$ and $Q_{ij}^*{}_{(b)}$ may be straight-forwardly computed once the $A_{ij}$ and $D_{ij}$ are found either by hand (see Appendixes A through C) for laminates having a few layers or by computer using the program SQ5 for laminates of many layers (see Appendix D). When using NASTRAN, the stiffnesses in Equation (E.8) are input to NASTRAN as the variables $G_{ij}$ on the MAT 2 cards, as previously indicated.
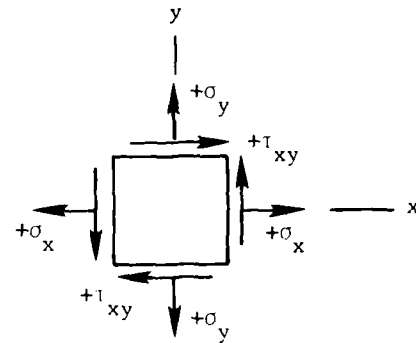
BLANK PAGE

## APPENDIX F

## PROCEDURE FOR DETERMINING TWO-DIMENSIONAL IN-PLANE LAMINA
## STRESSES BY POST-PROCESSING FINITE-ELEMENT OUTPUT

The following procedure is used to determine in-plane lamina stresses by post-processing the computer finite-element output.

1.  Determine the equivalent material stress on the upper (u) and lower (1) surface of the element from computer finite-element analysis output (use sign convention shown in sketch on right):

$$\sigma_{x_u} = \underline{\quad*\quad} \qquad \sigma_{x_1} = \underline{\quad*\quad}$$

$$\sigma_{y_u} = \underline{\quad*\quad} \qquad \sigma_{y_1} = \underline{\quad*\quad}$$

$$\tau_{xy_u} = \underline{\quad*\quad} \qquad \tau_{xy_1} = \underline{\quad*\quad}$$

2.  Decompose the surface stresses into membrane (m) and bending (b) components:

$$\left\{ \begin{array}{c} \sigma_x \\ \sigma_y \\ \tau_{xy} \end{array} \right\}_m = \frac{1}{2} \left\{ \begin{array}{c} \sigma_{x_u} \\ \sigma_{y_u} \\ \tau_{xy_u} \end{array} \right\} + \frac{1}{2} \left\{ \begin{array}{c} \sigma_{x_1} \\ \sigma_{y_1} \\ \tau_{xy_1} \end{array} \right\}$$

and

$$\left\{ \begin{array}{c} \sigma_x \\ \sigma_y \\ \tau_{xy} \end{array} \right\}_b = \frac{1}{2} \left\{ \begin{array}{c} \sigma_{x_u} \\ \sigma_{y_u} \\ \tau_{xy_u} \end{array} \right\} - \frac{1}{2} \left\{ \begin{array}{c} \sigma_{x_1} \\ \sigma_{y_1} \\ \tau_{xy_1} \end{array} \right\}$$

---

*Values from finite-element output.

75

3. Compute equivalent membrane and bending strains:

$$\left\{ \begin{array}{c} \varepsilon_x \\ \varepsilon_y \\ \gamma_{xy} \end{array} \right\}_m = \left[ \begin{array}{ccc} C_{11} & C_{12} & C_{16} \\ C_{12} & C_{22} & C_{26} \\ C_{16} & C_{26} & C_{66} \end{array} \right]_m \left\{ \begin{array}{c} \sigma_x \\ \sigma_y \\ \tau_{xy} \end{array} \right\}_m$$
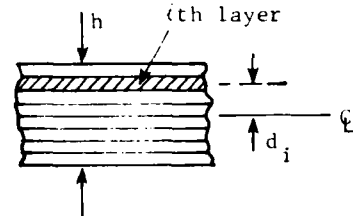
where $[C_{ij}]_m = [Q^*_{ij}]_m^{-1}$ (see Appendix E),

and

$$\left\{ \begin{array}{c} \varepsilon_x \\ \varepsilon_y \\ \gamma_{xy} \end{array} \right\}_b = \left[ \begin{array}{ccc} C_{11} & C_{12} & C_{16} \\ C_{12} & C_{22} & C_{26} \\ C_{16} & C_{26} & C_{66} \end{array} \right]_b \left\{ \begin{array}{c} \sigma_x \\ \sigma_y \\ \tau_{xy} \end{array} \right\}_b$$

where $[C_{ij}]_b = [Q^*_{ij}]_b^{-1}$ (see Appendix E).

4. Compute total strains in the i-th layer:

$$\left\{ \begin{array}{c} \varepsilon_x \\ \varepsilon_y \\ \gamma_{xy} \end{array} \right\}_i = \left\{ \begin{array}{c} \varepsilon_x \\ \varepsilon_y \\ \gamma_{xy} \end{array} \right\}_m + \frac{d_i}{h/2} \left\{ \begin{array}{c} \varepsilon_x \\ \varepsilon_y \\ \gamma_{xy} \end{array} \right\}_b$$



5. Compute the stress in the i-th layer in direction of the x and y axes:

$$\left\{ \begin{array}{c} \sigma_x \\ \sigma_y \\ \tau_{xy} \end{array} \right\}_i = \left[ \begin{array}{ccc} \overline{Q}_{11} & \overline{Q}_{12} & \overline{Q}_{16} \\ \overline{Q}_{12} & \overline{Q}_{22} & \overline{Q}_{26} \\ \overline{Q}_{16} & \overline{Q}_{26} & \overline{Q}_{66} \end{array} \right]_i \left\{ \begin{array}{c} \varepsilon_x \\ \varepsilon_y \\ \gamma_{xy} \end{array} \right\}_i$$

6. Compute the stress in the i-th layer in direction of "1" and "2" axes (where "1" makes an angle $\theta$ with the x axes):

$$\left\{ \begin{array}{c} \sigma_1 \\ \sigma_2 \\ \tau_{12} \end{array} \right\}_i = \left[ \begin{array}{ccc} \cos^2\theta & \sin^2\theta & 2\sin\theta\cos\theta \\ \sin^2\theta & \cos^2\theta & -2\sin\theta\cos\theta \\ \sin\theta\cos\theta & -\sin\theta\cos\theta & (-\cos^2\theta+\sin^2\theta) \end{array} \right]_i \left\{ \begin{array}{c} \sigma_x \\ \sigma_y \\ \tau_{xy} \end{array} \right\}_i$$
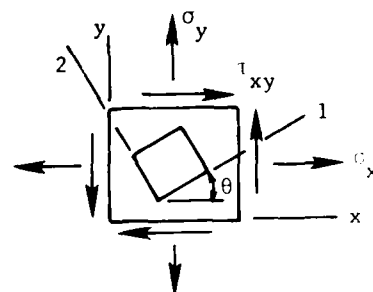
BLANK PAGE

# REFERENCES

1. Greszczuk, L.B. and M. Ashizawa, "Advanced Composite Foil Test Component (Tapered Box Beam)--Final Report," Contract N00024-74-C-5441, McDonnell Douglas Astronautics Company, Prepared by U.S. Naval Systems Command, May 1977.

2. Oken, S., "Development of an Advanced Composite Hydrofoil Flap--Phase II Final Design," The Boeing Co., Report D180-24630-1 (Apr 1978).

3. Greszczuk, L.B., "Elastic Constants and Analytical Methods for Filament Wound Shell Structures," Douglas Aircraft Co., SM45849 (Jan 1964).

4. Smith, C.S., "Calculation of Elastic Properties of GRP Laminates for Use in Ship Design," Symposium on GRP Ship Construction, London, October 1972.

5. Jones, R.M., Mechanics of Composite Materials, McGraw-Hill (1975).

6. Ashton, J.E. and J.M. Whitney, Theory of Laminated Plates, Tech. Publ. Co., Stamford, Conn. (1970).

7. Muha, T.J., "User's Manual for the Laminate Point Stress Analysis Computer Program SQ5 as Revised by AFFD/FBC," AFFDL-TM-74-107-FBC (Jul 1974).

8. Timoshenko, S. and S. Woinowsky-Krieger, Theory of Plates and Shells, McGraw-Hill (1959).

9. Handbook of Structural Stability, Edited by Column Research Committee of Japan, Corona Publ. Co., Ltd., Tokyo, Japan (1971).

10. Wong, D.K., "Finite Element Analysis of a Composite Box Beam," Master's thesis, Virginia Polytechnic University, May 1980.

11. The NASTRAN User's Manual (Level 16.0), Sci. and Tech. Info. Office, Natl. Aeronaut. and Space Admin., Wash., D.C., March 1976.

BLANK PAGE

# INITIAL DISTRIBUTION

| Copies | | Copies | |
|---|---|---|---|
| 1 | DDR&E/Lib | 1 | NAVSHIPYD LONG BEACH CA |
| 1 | CNO/OP 098T | 1 | NAVSHIPYD PEARL HARBOR HI |
| 1 | CNR/Code 474 | 1 | NAVSHIPYD PHILADELPHIA PA |
| 2 | CHNAVMAT | 1 | NAVSHIPYD PORTSMOUTH NH |
| | 1 MAT 08T23 | | |
| | 1 Lib | 1 | NAVSHIPYD PORTSMOUTH VA |
| 1 | USNA | 1 | NAVSHIPYD VALLEJO CA |
| 1 | NAVPGSCOL | 12 | DTIC |
| 1 | USNROTCU & NAVADMINU MIT | 1 | Wright-Patterson AFB |
| | | | Structures Div. |
| 1 | DNL | | |
| | | 3 | U.S. COGARD |
| 1 | NRL | | 1 Naval Eng Div. |
| | Tech Lib | | 1 Merchant Marine Tech |
| | | | Div. |
| 16 | NAVSEA | | 1 Ship Structures Comm |
| | 1 SEA 03R | | |
| | 1 SEA 312 | 1 | Lib of Congress |
| | 1 SEA 312 (Aronne) | | |
| | 1 SEA 32 | 2 | MARAD |
| | 1 SEA 32R (Pohler) | | 1 Div. of Ship Design |
| | 1 SEA 321 | | 1 Off of Res and Dev |
| | 1 SEA 322 | | |
| | 1 SEA 323 | 1 | NSF |
| | 1 SEA 323 (O'Brien) | | Engr Div Lib |
| | 1 SEA 323 (Arntson) | | |
| | 1 SEA 323 (Dye) | 1 | Univ of California, Berkeley |
| | 1 SEA 323 (Gallagher) | | Dept of Naval Arch |
| | 1 SEA 323 (Swann) | | |
| | 1 SEA 05R | 1 | Catholic Univ |
| | 1 SEA 05R (Vanderveldt) | | Dept Mech Engr |
| | 1 SEA 996 (Tech Lib) | | |
| | | 1 | George Washington Univ |
| 1 | NAVAIRSYSCOM | | School of Engr & |
| | Str Br (Code 5302) | | Applied Sci |
| 1 | NAVOCEANSYSCEN | 1 | Lehigh Univ/Dept Civil Engr |
| 1 | NAVSHIPYD BREMERTON WA | 1 | Mass Inst of Tech |
| | | | Dept Ocean Engr |
| 1 | NAVSHIPYD CHARLESTON SC | | |

| Copies | | Copies | Code | Name |
|---|---|---|---|---|
| 1 | Univ of Michigan<br>Dept NAME | 1 | 1770 | |
| | | 1 | 1770.7 (m) | |
| 1 | Southwest Res Inst | 1 | 185 | |
| 1 | Stevens Inst Tech<br>Davidson Lab | 1 | 281 | |
| 1 | Virginia Poly Inst &<br>State Univ/Dept<br>Engr Mech | 10 | 5211.1 | Reports Distribution |
| | | 1 | 522.1 | Unclassified Lib (C) |
| | | 1 | 522.2 | Unclassified Lib (A) |
| 1 | Webb Inst | | | |
| 2 | National Academy of Sci<br>1  National Res Council<br>1  Ship Hull Res Comm | | | |
| 1 | SNAME | | | |
| 1 | American Bureau of Shipping | | | |

CENTER DISTRIBUTION

| Copies | Code | Name |
|---|---|---|
| 1 | 11 | |
| 1 | 1605 | |
| 1 | 17 | |
| 1 | 1706 (m) | |
| 1 | 1720 | |
| 1 | 1730 | |
| 1 | 1730.1 | |
| 1 | 1730.2 | |
| 1 | 1730.3 | |
| 1 | 1730.4 | |
| 25 | 1730.5 | |
| 1 | 1730.6 | |
| 1 | 1740 | |
| 1 | 1750 | |